ABSTRACT

DEVELOPMENT OF A MULTI-LEAD TRANS-THORACIC IMPEDANCE PNEUMOGRAPH FOR HEART RATE VARIABILITY STUDIES

by
Curtis Bashford

In this study, a device that measures respiratory tidal volume and ECG for use in heart rate variability studies, was designed, built and tested. The device developed is a Multi-Lead Trans-Thoracic Impedance Pneumograph, which determines tidal volume on a breath by breath basis, utilizing both hardware and software. It uses standard ECG electrodes which provide increased comfort and mobility to the subject over traditional spirometry methods. The device operates similar to traditional bipolar impedance pneumographs except that instead of only one lead (electrode pair), four leads are acquired simultaneously using time-division multiplexing; providing data from different locations and vectors on the subjects chest.

Respiration, ECG and spirometry data were collected using the device from 6 normal, healthy subjects for several trials of normal and paced breathing. Results were correlated against the spirometry data to determine whether sufficient data are provided by the four leads and also to determine the accuracy of the device. It was concluded that combining data from all 4 leads using generalized additive modeling results in correlations in the range of 0.8 - 1.0, but more investigation is needed to determine usefulness in actual HRV applications.

DEVELOPMENT OF A MULTI-LEAD TRANS-THORACIC IMPEDANCE PNEUMOGRAPH FOR HEART RATE VARIABILITY STUDIES

by
Curtis Bashford

A Thesis
Submitted to the Faculty of
New Jersey Institute of Technology
in Partial Fulfillment of the Requirements for the Degree of
Master of Science in Biomedical Engineering

Biomedical Engineering Committee

January 1995

Blank Page

APPROVAL PAGE

DEVELOPMENT OF A MULTI-LEAD TRANS-THORACIC IMPEDANCE
PNEUMOGRAPH FOR HEART RATE VARIABILITY STUDIES

by
Curtis Bashford

Dr. Stanley Reisman, Thesis Advisor   Date
Professor of Electrical Engineering and Biomedical Engineering, NJIT, NJ

Dr. David Kristol, Committee Member   Date
Director of Biomedical Engineering program, NJIT, NJ

Dr. Peter Engler Committee Member   Date
Associate Professor of Electrical Engineering and Biomedical Engineering, NJIT, NJ

BIOGRAPHICAL SKETCH

Author: Curtis Bashford

Degree: Master of Science in Electrical Engineering

Date: January, 1995

Undergraduate and Graduate Education:

- Master of Science in Biomedical Engineering
  New Jersey Institute of Technology,
  Newark, NJ, 1995

- Bachelor of Science in Electrical Engineering
  New Jersey Institute of Technology,
  Newark, NJ, 1987

- Associates of Arts in Engineering
  Union County College,
  Cranford, NJ, 1984

Major: Biomedical Engineering

Professional Background:

General Devices, Ridgefield, NJ 1987 - Present
   Manufacturers of medical electronics
   Engineer involved in the development of medical electronics for the EMS
   marketplace.

This thesis is dedicated to my wife Amanda and my son Scott,
for their support and understanding during the many long hours when time that
could have been spent together was sacrificed so that I may do this work.

ACKNOWLEDGMENT

TABLE OF CONTENTS

TABLE OF CONTENTS
(Continued)

Chapter   **Page**

LIST OF TABLES

LIST OF FIGURES

LIST OF FIGURES
(Continued)

CHAPTER 1

BACKGROUND

1.1 Introduction

This thesis involves the measurement of physiological signals and quantities. Knowledge of both engineering and physiology are combined in an attempt to move one step closer to understanding and solving one of the many unknowns of the workings of the human body. This chapter contains background information that forms the foundation upon which the thesis is based.

1.2 Objective

The objective of this thesis is to design, build and test a device that can be used to measure both electrocardiogram (ECG) and respiratory tidal volume. This study is part of ongoing research in heart rate variability (HRV) at the Kessler Institute for Rehabilitation in West Orange NJ. For the HRV studies it is desired to be able to measure respiratory tidal volume by a method that does not restrict motion, cause discomfort or cause the subject to be overly conscious of the breathing effort. Traditional spirometry provides accurate measurements, but can cause discomfort when used for any length of time, limits motion and inherently makes the subject very conscious of their breathing effort.

Since it is necessary to acquire the patients ECG, it was decided to use transthoracic (across the thorax or chest) impedance pneumography which also connects to a

subject using only electrodes and lead wires. Trans-thoracic impedance (TTI) pneumography is a technique that has been used for years to determine respiration rates, but has had only limited success for measuring respiratory volumes consistently. Prior research has shown that different electrode placements yield varied results and that there is no one optimal position for different subjects or even for different breathing patterns in any one subject [3], [8]. Based on this it was decided to develop a device that can acquire respiration data from multiple leads or electrode pairs (thus the name Multi-Lead) positioned around the patients chest simultaneously in the hopes that there is enough information in the data to accurately determine tidal volume under varied conditions. To evaluate the performance of the device, data would also be acquired from a spirometer so that the results could be correlated and accuracy accessed. The device developed in this study is a Multi-Lead Trans-Thoracic Impedance Pneumograph, which determines tidal volume on a breath by breath basis, utilizing both hardware and software. If successful, the intended operation would be such that a spirometer would only be used at the beginning of a clinical trial for calibration purposes, after which the multi-lead TTI pneumograph would acquire ECG and respiration data and the tidal volumes be determined.

1.3 The Heart and the Electrocardiogram

The heart is a muscular organ located in the chest (thoracic) cavity and enclosed in a fibrous sac, the pericardium. The heart is divided longitudinally into right and left halves, each consisting of two chambers, an atrium and a ventricle [15]. The heart is actually two

separate pumps, a right heart that pumps the blood through the lungs and the left heart

that pumps the blood through the peripheral organs as shown in Figure 1.3.1 [2].
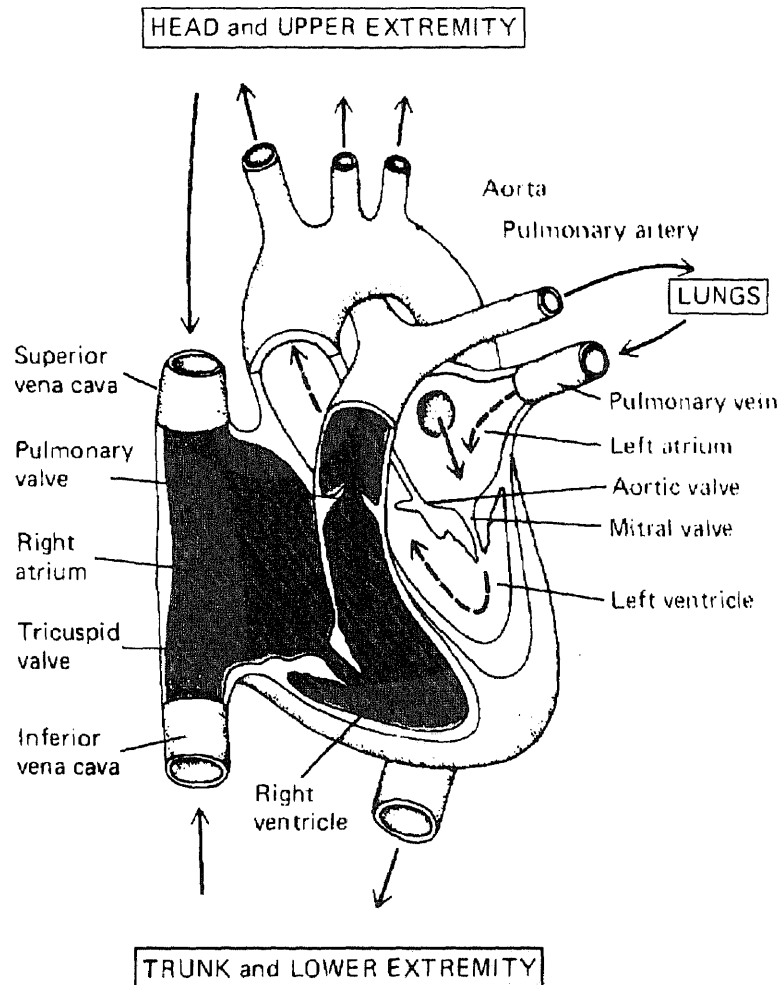
Figure 1.3.1 Structure of the heart and course of blood flow through the chambers [2].

The pumping action for each heart beat or cardiac cycle, is initiated and controlled

by an organized sequence of electrical activity through a specialized excitatory and

conducting system. The conducting system of the heart is shown in figure 1.3.2. The

origin of the heart beat is a small strip of specialized muscle in the anterosuperior wall of

the right atrium called the sinoatrial (S-A) node. The S-A node is refereed to as the pacemaker of the heart because it contains cells that are autorhythemic, i.e. they are capable of autonomus rhythmical self-excitation. The inherent rhythm of the S-A node is approximately 100 beats per minute (BPM). The heart is provided with a rich supply of both sympathetic and parasympathetic nerves which serve to control heart rate by modifying the inherent rhythms of the S-A and atrioventricular (A-V) nodes. Sympathetic stimulation has the effect of increasing heart rate while parasympathetic stimulation has the opposite effect and tends to slow heart rate. This neural intervention is of interest for heart rate variability (HRV) studies.

Internodal
pathways

S-A node

A-V node

A-V bundle

Left bundle
branch

Right bundle
branch
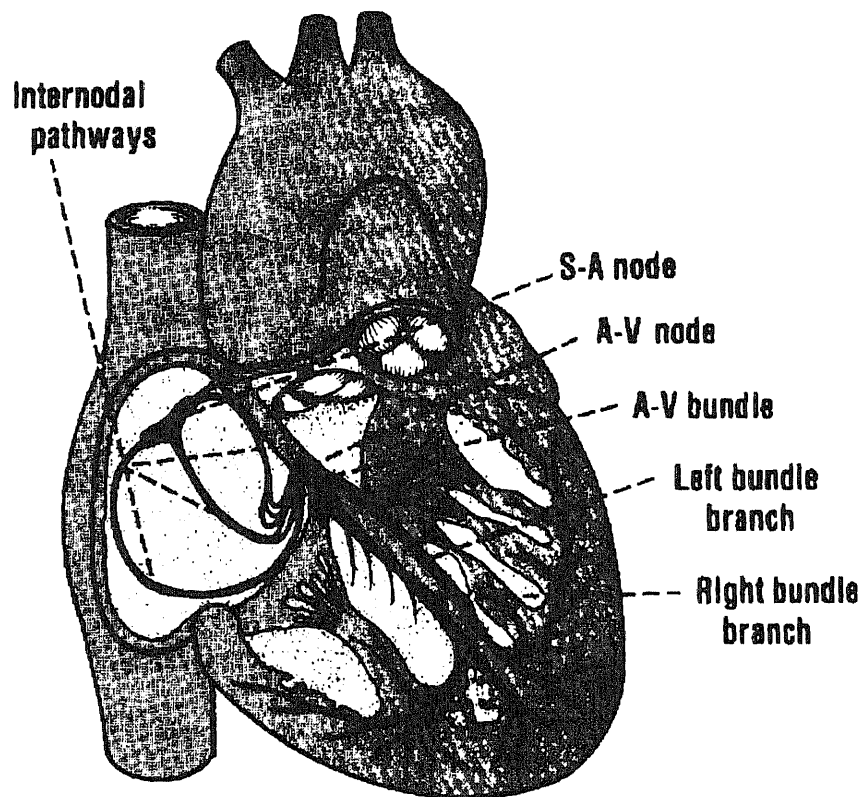
Figure 1.3.2 Conducting system of the heart [2].

Action potentials that are generated in the S-A node trigger the sequence of electrical activity that cause a heart beat. From the S-A node, the wave of excitation spreads over the atria, causing them to contract and through the internodal pathways to the A-V node at the base of the right atrium. The only electrically conductive path between the atria and ventricles is through the A-V node. Once at the A-V node the signal is delayed by approximately 0.1 second and is then enters the ventricles via the bundle if His. It is then spread rapidly down the right and left bundle branches to the Purkinje fibers which spread the signal to all parts of the ventricles, causing the ventricles to contract.
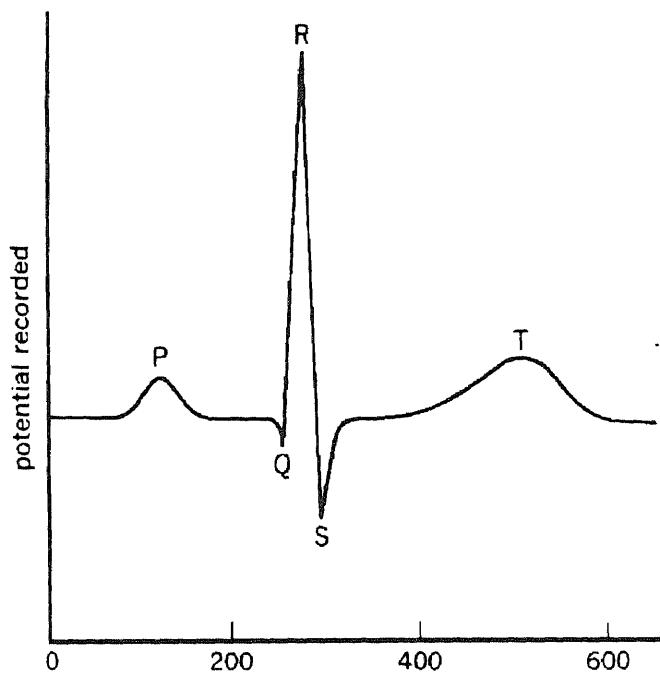
Figure 1.3.3 The normal electrocardiogram (ECG) [2].

The spread of the electrical activity throughout the cardiac tissue can be detected and recorded at the surface of the skin as a sum of many action potentials and is refereed to as the electrocardiogram (ECG). The normal ECG shown in figure 1.3.3 is composed of a P wave, a "QRS complex," and a T wave. The QRS complex is often three separate waves, the Q wave, the R wave, and the S wave [2]. The P wave is caused by electrical currents generated as the atria depolarize prior to contraction, and the QRS complex is caused by electrical currents generated as the ventricles depolarize. The T wave is generated as the ventricles repolarize. Repolarization of the atria is masked by the QRS complex. The rates of conduction can be seen by observing the ECG. The PQ interval represents the delay at the A-V node. The Q-R interval identifies the ventricular depolarization phase as being fast and strong, while the ventricular repolarization shown by the T wave is much slower.

The electrical connections for the standard bipolar limb leads is shown in figure 1.3.4. The limb leads are bipolar in that the ECG is recorded from two specific electrodes on the body. The ECG is typically recorded using silver-silver-chloride type surface electrodes. The limb leads use three electrodes placed on the body (or chest) and are referred to by their placement as right arm (RA), left arm (LA) and left leg (LL). Often a ground or guard electrode is applied to the right leg (RL).

This configuration of electrodes provides for ECG measured from three leads (electrode pairs), lead I, lead II and lead III. Lead I is measured with the negative terminal at RA and the positive at LA. Lead II is measured with the negative terminal at RA and the positive at LL and lead III is measured with the negative terminal at LA and the

positive at LL. Each lead provides a different vector or electrical view of the heart. Lead II is commonly used for monitoring because it provides the largest QRS of the three leads and it is of positive polarity. Devices for the recording of ECG are specialized high gain amplifiers with a means for recording or displaying the amplified signal. Since the amplitude of a typical lead II QRS is only 1mV special attention must be given to noise rejection.
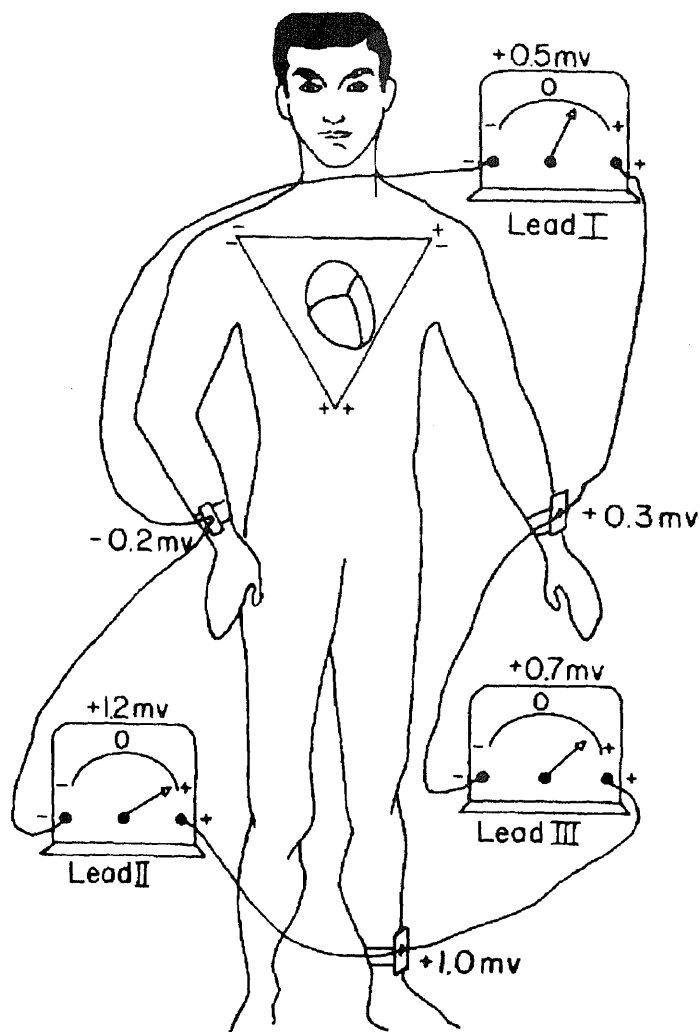
Figure 1.3.4 Conventional arrangement of electrodes for recording of the standard electrocardiogram (ECG) [2].

In this study, only a lead II ECG is acquired. This is all that is necessary for HRV studies since lead II provides a large QRS and the only information required is accurate detection of the R wave (peak of the QRS). A detailed description of the circuitry used to acquire the ECG is provided in chapter 2.

1.4 Heart Rate Variability Studies

Heart rate is the rate at which the heart repeats it's pumping cycles and is typically expressed in beats per minute (BPM). By observing electrical activity of the heart with surface electrodes and viewing the electrocardiogram or ECG, the different waveforms that occur for each cardiac cycle (heart beat) can be seen; P-wave, QRS complex and T-wave. The standard method of heart rate measurement is to detect the R-waves and determine the average count over some fixed time frame. If the R-R intervals (time between successive beats) are measured accurately, it can be observed that there is variability in heart rate. The basis for heart rate is the intrinsic pacemaker of the sinoatrial node. This pacemaker action is modified by neurohumoral mechanisms since the heart receives a rich supply of parasympathetic and sympathetic neural fibers. The fluctuations in heart rate, known as heart rate variability, discloses activities of both the parasympathetic and sympathetic nervous systems. Generally, sympathetic input increases heart rate while parasympathetic input decreases it[18]. Investigation of these neural control mechanisms is the basis for heart rate variability (HRV) studies.

A HRV signal can be formed by transforming R-R intervals into a time series. As noted by Kamath and Fallen [7], only through a transformation of the time series events to

the frequency domain can one appreciate the existence of physiological rhythms oscillating at specific frequencies. Over the last 20 years, the power spectrum (PS) has come to dominate the quantitative methods. The heart rate power spectrum has been found to be an effective noninvasive measure for studying neural modulation of the heart in a variety of clinical and research settings [17]. The power spectrum analysis of heart rate PS-HRV yields three major bands. A low-frequency peak that appears within the spectral band ranging from 0.06 to 0.15 Hz is associated with baroreceptor-mediated blood pressure control. A high-frequency peak in the range 0.15 to 0.4 Hz is strongly correlated with respiratory sinus arrhythmia. A very-low-frequency peak below 0.05 Hz has been linked with vasomotor control and/or temperature control [7], [18]. Figure 1.4.1 shows the spectrum of inter-beat intervals (IBI) from a subject, in which there is a peak at the respiration frequency.
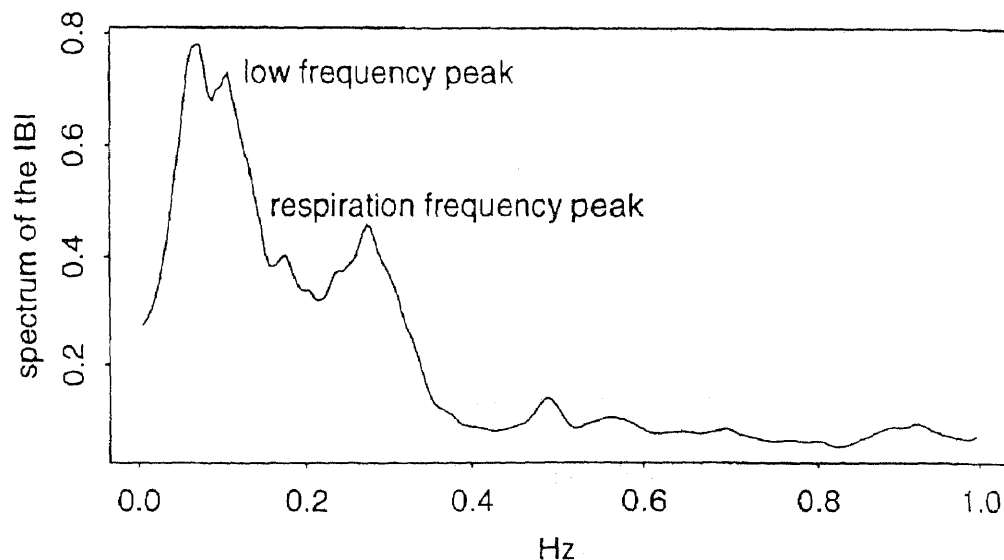
Figure 1.4.1 A spectrum of a heart rate variability signal [18].

Zhang [18] has noted that respitation-asscoiated heart rate variability (RA-HRV) has recently become a topic of considerable interest for investigations of normal physiology and disease because the potential utility of RA-HRV as an index of vagal effects on the heart assumes special importance in understanding of the complexities of autonomic control. It is known that inspiration increases heart rate and expiration decreases heart rate. Conventional time-series techniques such as power spectrum analysis and complex demodulation have been used to quantify RA-HRV. Power spectrum analysis separates the power on the basis of the frequency components in the interbeat intervals. Complex demodulation enables the amplitude and phase of respiration frequency components to be displayed as functions of time [18].

Since the present study is part of ongoing research in HRV, its purpose is to develop a device that measures both ECG and respiratory tidal volume, ultimately to be used for HRV studies. The respiration measurement technique selected is impedance pneumography. This method was selected in part because it complements the HRV methods since both impedance pneumography and ECG use electrodes. Impedance pneumography also allows greater comfort and less restriction for the subject as opposed to using a spirometer for respiration measurements.

1.5 Respiratory Measurements

The process of respiration can be divided into four major mechanistic events: (1) pulmonary ventilation, which means the inflow and outflow of air between the atmosphere and the lung alveoli, (2) diffusion of oxygen and carbon dioxide between the alveoli and

the blood, (3) transport of oxygen and carbon dioxide in the blood and body fluids to and from the cells, (4) regulation of ventilation and other facets of respiration [2]. Within the scope of this study we are concerned only with the first of these aspects and only as it pertains to lung volumes and their measurement.
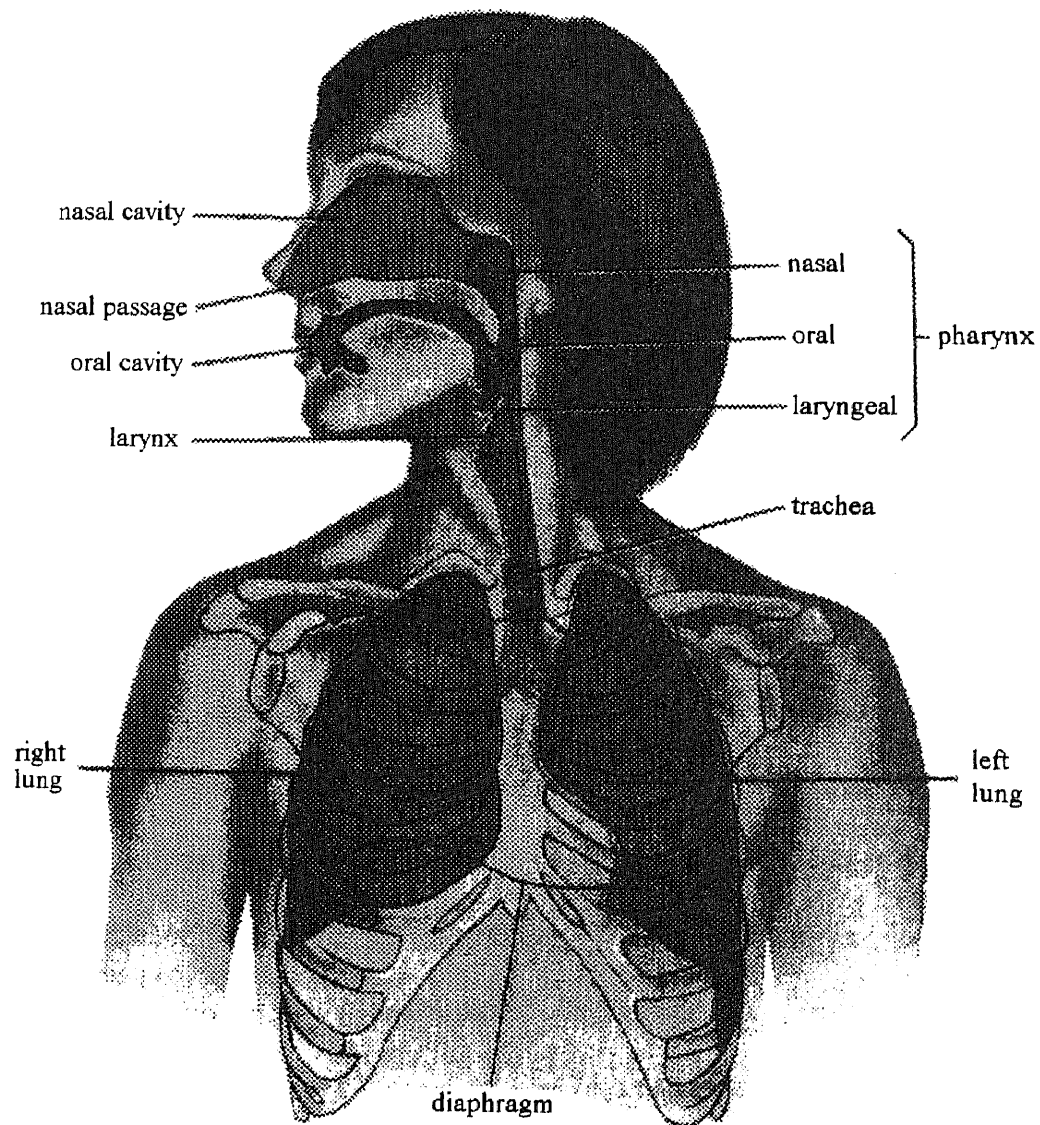
Figure 1.5.1 Organization of the respiratory system [15].

The respiratory system as shown in figure 1.5.1 comprises the lungs, the series of airways leading to the lungs, and the chest structures responsible for movement of air in and out of the lungs. The thoracic cavity is filled by the lungs together with the heart, great vessels, esophagus, thymus and certain nerves. The lungs are not simply hollow balloons but have a highly organized structure consisting of air-containing sacs and tubes, blood vessels, and elastic connective tissue [15]. The conducting portion of the respiratory system is composed of a series of branching tubes that begin at the nose and mouth and continually branch and become smaller until they finally terminate in the sacs called the alveoli. The alveoli are surrounded by capillaries, the total area of which is approximately $135m^2$ or roughly 80 times the external surface area of the body. This immense interface between the alveoli and capillaries is the site where gas exchange takes place.

To exchange air, the lungs can be expanded and contracted in two ways: (1) by downward and upward movement of the diaphragm to lengthen or shorten the chest cavity, and (2) by elevation and depression of the ribs to increase and decrease the anteroposterior diameter of the chest cavity [2]. Figure 1.5.2 demonstrates how the muscular movements (diaphragm, abdominal and intercostal) change the dimensions of the chest cavity during inspiration and expiration. Alveolar pressure changes are caused by these dimensional changes of the lungs. Air moves into (inspiration) and out of (expiration) the lungs because the alveolar pressure is made, alternately, less than and greater than atmospheric pressure [15].

EXPIRATION INSPIRATION

Increased vertical diameter

Increased A-P diameter

External intercostals contracted

Internal intercostals relaxed

Elevated rib cage

Abdominals contracted

Diaphragmatic contraction
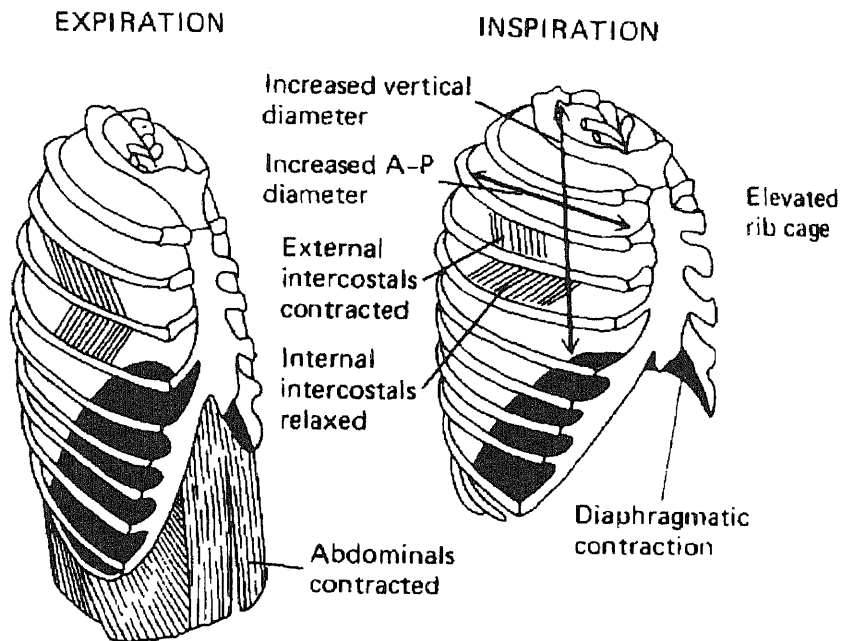
Figure 1.5.2 Expansion and contraction of the thoracic cage during expiration and inspiration, illustrating especially diaphragmatic contraction, elevation of the rib cage, and function of the intercostals [2].

The volume movement of air into and out of the lungs can be recorded using a process called spirometry. There are many types of spirometers, most of which generate a tracing or output signal as a subject breaths into a tube connected to a gas chamber. The spirometer tracing shown in figure 1.5.3 shows changes in lung volume under different conditions of breathings. From the figure it can be seen that there are four volumes and four capacity regions identified, which are defined and typical volumes indicated as follows:

- Tidal volume is the volume of air inspired or expired with each normal breath, ≈ 500 mL.

- Inspiratory reserve volume is the extra volume of air that can be inspired over and beyond the tidal volume, ≈ 3000 mL.

- Expiratory reserve volume is the volume of air that can still be expired by forceful expiration at the end of a normal tidal expiration, ≈ 1100 mL.

- Residual volume is the volume of air remaining in the lungs after the most forceful expiration, ≈ 1200 mL.

- Inspiratory capacity equals the tidal volume plus the inspiratory reserve volume, ≈ 3500 mL.

- Functional residual capacity equals the expiratory reserve volume plus the residual volume, ≈ 2300 mL.

- Vital capacity equals the inspiratory reserve volume plus the tidal volume plus the expiratory reserve volume, ≈ 4600 mL.

- Total lung capacity is equal to the vital capacity plus the residual volume, ≈ 5800 mL.
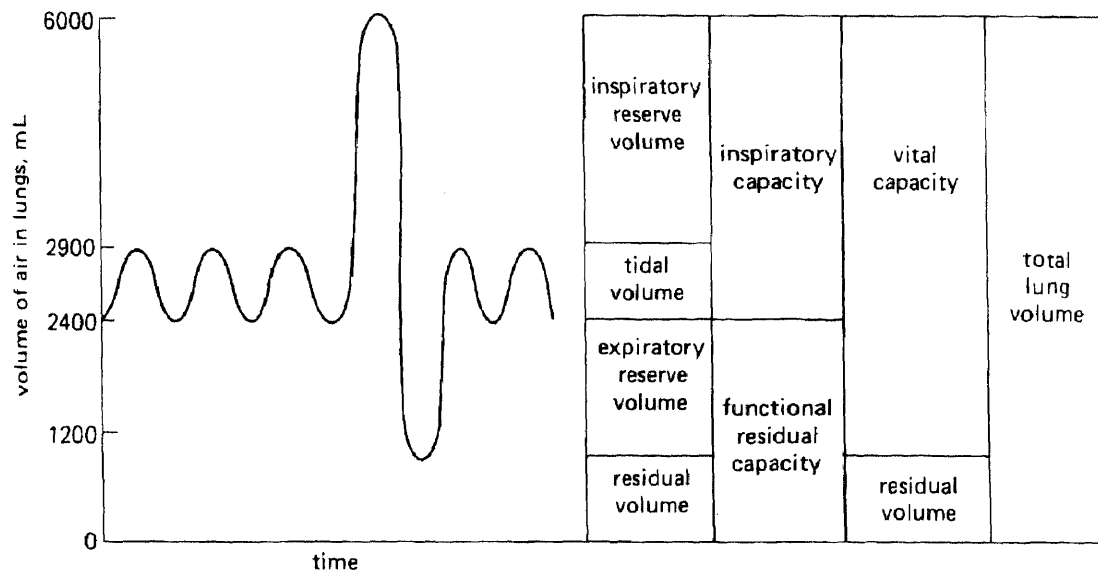
Figure 1.5.3 Lung volumes and capacities as measured on a spirograph. When the subject inspires the pen moves up; with expiration it moves down [15].

Another respiratory term, minute volume, is the total amount of new air moved into the respiratory passages each minute, and this is equal to tidal volume times the respiratory rate.

For heart rate variability studies, the only respiratory measurement of interest is tidal volume. Traditionally these measurements are performed with a spirometer. Spirometry provides accurate results but requires the subject to wear a face mask with connective tubing which is uncomfortable for long term use and restricts motion. In the following chapters the development of an alternate method of tidal volume measurement, Multi-lead trans-thoracic impedance pneumography, is discussed in detail.

1.6 Impedance Pneumography

Impedance pneumography is an indirect technique for the continuous, dynamic measurement of respiratory volume. The impedance pneumograph is a specialized type of impedance recorder and measures respiration through the relationship between thoracic electrical impedance and respiratory volume [10]. The basic quantity measured by the impedance pneumograph is trans-thoracic electrical impedance change [10]. The measurements are trans-thoracic in that the impedance is measured across the thoracic cavity or chest of a subject. The impedance pneumograph operates on the concept that trans-thoracic impedance changes in proportion with changes in the geometry of the thoracic cavity that occurs with breathing. Typically, on inspiration the diaphragm lowers, the lungs fill with air and the chest expands resulting in an increase in impedance. As stated by Hamilton [3] and Wadhwani et. al.[16], trans-thoracic impedance measurements

of tidal volume have been studied by many investigators, but there is a lack of agreement about the nature of the impedance signal associated with breathing. Possible sources of the impedance changes that have been cited by investigators include artifact at the electrode-skin interface, current flow through the posterior path of the thorax and changes deep within the chest. As noted by Nyboer[9], bioelectric impedance has a frequency dependent component as related to reactive impedance. Capacitive impedance is present at audio and intermediate radio frequencies at the boundaries of cells. Above 5MHz, the membranes of cells are well shunted to the extracellular matter and other cells.

Studies dating back to the early 1900's by researchers such as Cremer (1907), Atzler (1935), Fenning (1937) and Nyboer et. al.(1940) have documented thoracic dielectric changes. Early instrumentation techniques included modulated oscillator and bridge circuit approaches. The most common of recent approaches is the constant current pneumograph. This technique uses a constant current AC voltage that is passed through the subject so that the peak to peak carrier voltage amplitude across the subject is proportional to the magnitude of the subject impedance. Any variation in the impedance magnitude causes modulation of the carrier amplitude. The impedance information is recovered by a demodulator such that the output signal is proportional to changes in the magnitude of the subject impedance[10]. The frequency of the constant current signal that is applied to the electrodes is typically 50-100KHz. The high frequency is necessary for two reasons, to reduce effects caused by contact impedance at the electrode to skin interface, and to preclude the possibility of subject stimulation. Furthermore, frequencies above 100KHz are not practical because of hardware constraints. Research done by

Rosell et. al.[11], shows that skin impedance at a frequency of 1Hz, can vary anywhere from 10KΩ to 1MΩ for measurements at various sites on the chest. It was also noted that the impedance becomes relatively constant at high frequencies for the different sites; about 200Ω at 1KHz and 120Ω at 1 MHz. Pacela [10], recommends a constant-current value on the order of 0.1 to 1.0 mA p-p.

As discussed by Hamilton[3], Hua et. al.[6], Luo et. al.[8], Pacela[10], Sahakian et. al.[12], there are two basic electrode systems that have been used in bioimpedance measurements. These are the four-electrode (tetrapolar) and two-electrode (bipolar) configurations, shown in figures 1.6.1 and 1.6.2 respectively. Both systems offer unique advantages [10].
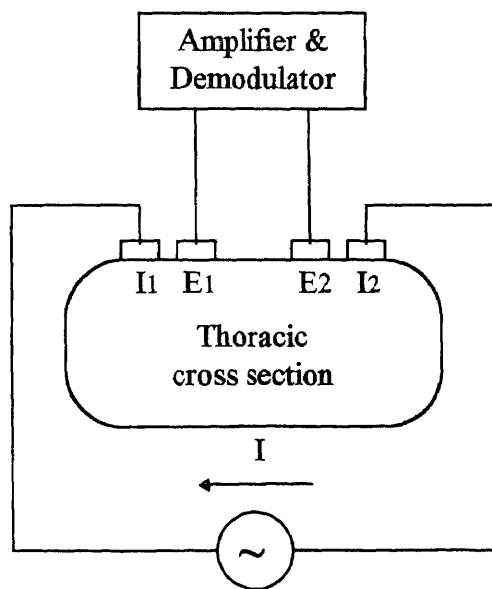
Figure 1.6.1 Tetrapolar electrode system.   Figure 1.6.2 Bipolar electrode system.
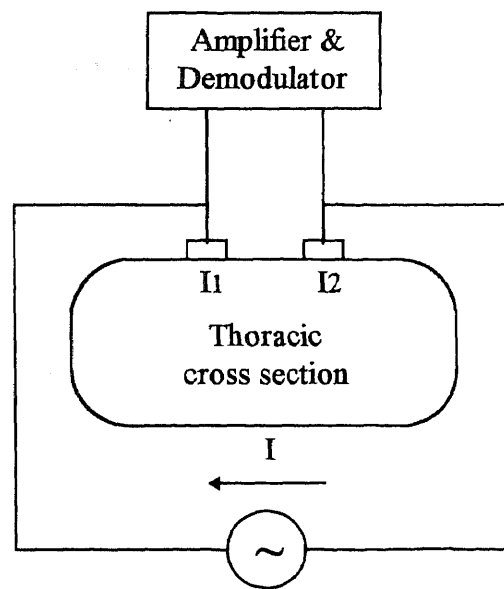
In the tetrapolar electrode system, the carrier oscillator signal (current) is applied to one pair of electrodes (I1 and I2) and the desired voltage signal is measured at the second pair of electrodes (E1 and E2). This scheme offers superior rejection of noise due to motion artifacts since changes in impedance at the electrodes does not significantly affect the signal voltage. In the bipolar electrode system, the carrier oscillator signal (current) and the desired voltage signal is applied to the same pair of electrodes (I1 and I2). While this system is more sensitive to motion artifact noise, it is simpler and less restrictive because there are less electrodes on the subject. Another approach to noise reduction is the addition of a guard ring around the electrodes or the use of a unilateral guard. As noted by Sahakian et. al.[12], applications that include ECG monitoring may already have a reference electrode and therefore no additional electrodes or connections are required to provide a unilateral guard. It was concluded by Cheng et. al.[1] that in multiple electrode systems, current should be applied and voltage measured from all available electrodes.

Electrode type and placement are important considerations for volumetric measurements. A comprehensive study by Luo et. al.[8] evaluates several electrode types and sizes in addition to comparing electrode placements. They concluded that the electrodes should meet the following requirements: low baseline impedance, high adhesion, high physical stability, thin electrode with high flexibility and an optimal electrode size of 70cm^2. Electrode placement was evaluated for 171 electrode pair combinations for optimal signal to artifact ratios, based on 32 electrodes placed evenly around the body trunk at four levels. Electrode placement locations suggested for multiple electrode measurements are shown in figure 1.6.3. As noted by Hamilton[3], the

greatest sensitivity for the impedance signal is seen with the electrodes placed at about the

eighth intercostal space, but is linear only at higher levels. Commonly used placement for

two electrode systems for respiration measurements is at the fourth intercostal space in

line with the nipples on the mid-axillary lines.
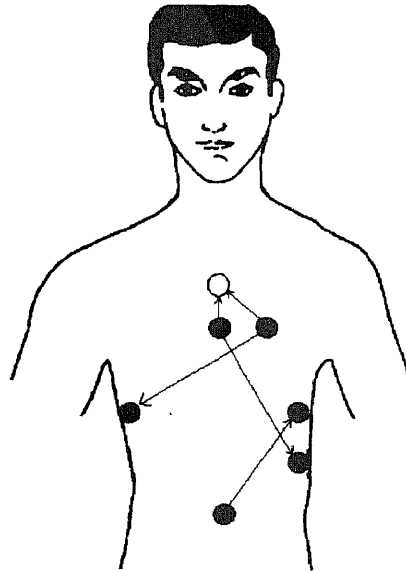
Figure 1.6.3 Suggested electrode placement locations for multiple electrode
measurements [8].

In this study a variation on traditional impedance pneumography methods is

discussed (Multi-lead TTI pneumography). This method involves bipolar impedance

measurements from four electrodes using time-division multiplexing. The multiplexing

allows 4 separate channels or leads to be simultaneously acquired. By having 4 leads of

respiration, measurements from 4 different positions on the thorax are provided in the

hopes that the data may be combined such that respiratory tidal volume may be

determined with accuracy and consistency that is superior to that of single lead impedance

pneumography.

1.7 Prior Research

As already noted by Hamilton[3], trans-thoracic impedance measurements of tidal volume have been studied by many investigators. Results of the study by Hamilton [3] showed errors of the system on the order of +/- 10% for both adults and infants as long as the subject is quiet and inactive. These findings are typical of attempts at impedance pneumography for volumetric measurements. It is also generally accepted that there is no one optimal electrode placement for all subjects and that calibration is necessary for each subject. Typically these measurements are evaluated by comparison with readings from a spirometer. Hansen et. al.[4], [5] suggests and demonstrates connecting the output of a spirometer to an analog to digital (A/D) converter and inputting the data into a personal computer. This allows for easy post processing of the data and comparison with other measurement techniques.

This study is part of ongoing research at Kessler Institute for Rehabilitation in West Orange. Prior research done by Seshadri [13] and others provided background information on signal processing methods and correlation of impedance pneumograph and spirometer data. In Seshadri's study, data from a spirometer and from two impedance pneumograph devices were evaluated quantitatively using linear and nonlinear regression algorithms. Several of the suggestions of Seshadri's work are addressed in this study namely; investigation of a multiple electrode system to acquire data for different electrode positions simultaneously, and combining data from different electrode positions in such a way to improve the correlations. Insight to the use of modeling techniques was obtained from the work of Sheshadri [13] and Zhang[18] and is later discussed in chapter 3.

CHAPTER 2

HARDWARE DEVELOPMENT AND EQUIPMENT

2.1 System Requirements

2.1.1 Overview

The stated objective of this thesis is the development of a device that acquires both ECG and respiration data for use in heart rate variability (HRV) studies. The front-end circuitry is the core of this device, which when used in conjunction with the data acquisition software provides the data for collection and processing. The front-end circuitry interfaces the human body to the data acquisition card, and was designed specifically for this thesis. In addition to the bio-potentials measured on the body, the output of a spirometer was to be interfaced to the data acquisition card for calibration and validation of the TTI pneumograph readings. Design criteria included the number of channels, sampling rates, bandwidth, isolation, power, and A/D card interfacing.

Although it is necessary to minimize the number of electrode/leads that connect to the patient for comfort and simplicity, it was determined that a total of seven would be required. Four leads of respiration were to be acquired using a time-division multiplexing scheme. A bipolar impedance measurement configuration was chosen, and therefore, at least four electrodes were required for respiration alone. Three more electrodes would be required, two for ECG and one for guard.

2.1.2 Specifications

The following is a list of the specifications to which the front-end hardware was designed and built:

CHARACTERISTIC   SPECIFICATION

TTI Pneumograph Front End
    Oscillator frequency.............................50KHz
    Inputs...Four bi-polar electrode pair positions RA-LA (leadI), RA-LL (lead II), LA-LL (lead III), and LL-RL (lead IV) utilizing standard silver-silver-chloride ECG electrodes.
    Outputs...One scope (multiplexed) BNC connector, four Respiration A/D channels, Biploar +/-5V.
    Bandwidth...0.1 to 25 Hz

ECG Front End
    Inputs...One differential electrode pair RA-LL (lead II)utilizing standard silver-silver-chloride ECG electrodes.
    Outputs...One scope, one ECG A/Dchannel, Biploar +/-5V.
    Bandwidth...0.5 to 100 Hz
    Gain...X1000 (1V=1mV RTI)

Spirometer Front End
    Inputs...Both potentiometer and TTL output types.
    Outputs...One spirometer A/Dchannel, Biploar +/-5V.
    Bandwidth...DC to 50 Hz

Event Marker ....Momentary switch closure, TTL.

Isolation/Protection ....Less than 100uA leakage current between patient connections and other equipment (computer/ACline)   and defibrillation protection as per AAMI standards.

Connectors
    Patient Cable....................................AAMI standard 6-pin patient cable.
    Spirometer POT/TTL........................3.5mm stereo / 3.5mm mono phone jacks.
    Event Marker ....3.5mm mono phone jack.
    Scope ECG/RESP out.......................BNC female / BNC female.

```
Battery..................................................1.3mm DC jack.
Charger................................................2.5mm DC jack
CIO-DAS08 analog/digital...................DB37 female / DB37 male
```

Indicators
```
Battery Power....................................Red LED
Computer Power................................Red LED
```

```
Logic control.............................................TTL from CIO-DAS08
Power control............................................Toggle switch, DPDT
Battery.....................................................12.0V, 1.0AH NICd
```

2.2 Front End Design

2.2.1 Number of Channels

In designing the front end circuitry to meet the system specifications, the number of channels was an important consideration because it directly affects the amount of hardware required. This is most evident when the isolation circuitry required per channel is considered. In order to minimize the number of channels, a multiplexing scheme was devised by the author in which the four respiration leads (channels) are time division multiplexed onto one channel for A/D conversion. This scheme resulted in a significant reduction in hardware and isolated power requirements by requiring only two channels to cross the isolation barrier, the multiplexed respiration channel and the ECG channel. The spirometer had no electrical connections or risk current paths with the patient and therefore was able to be connected through a non-isolated channel. A total of three signal channels (one with four sub-channels) are output by the front end for analog to digital conversion by the CIO-DAS08 data acquisition card.

2.2.2 Sampling Rates

Sampling rate requirements dictated the bandwidths of the front end circuitry. A different sampling rate was chosen for each of the acquired signals based on their specific requirements. The software used for data acquisition limits the maximum trial run time because of the fixed size memory array utilized. Therefore sampling rates chosen were optimized to allow the maximum length trial run while retaining sufficient signal integrity.

For heart rate variability studies, the ECG waveform is not important, but accurate peak detection is required. The ECG sampling rate was chosen to be 200Hz. This rate provides both good waveform reproduction and a resolution of 5mS for peak detection. This resolution allows accurate peak detection for ECG up to a rate of 120 beats per minute (BPM) since the R-R interval (time interval from R wave to R wave of successive beats) difference for rates above 120 is less than 5mS. The scope of this study would not involve heart rates above 120 BPM, typical rates being within the range of 60-100 BPM.

The respiration sub-channels were sampled at 25Hz each which is more than high enough since most of the frequency content of respiration signals is below 10Hz. For paced breathing as in this study, the respiration signal is quasi-sinusoidal with a frequency range of 0.1 to 0.4 Hz corresponding to 6 to 24 breaths per minute. The composite respiration channel operates at a 100Hz rate (25Hz per sub-channel with four sub-channels).

In order to determine the sampling rate required for the TTL spirometer signal, the maximum expiration rate had to be considered (refer to section 2.5 for a detailed description of the spirometer). A realistic maximum rate was determined experimentally

as 2.5L per second which is a much higher rate than will be achieved in this study. The maximum signal transition rate is therefore 2.5 L/sec divided by 0.05L/transition which gives 50 transitions/sec. max.. Since the signal is either TTL high or Low, only one sample is required to determine the logic state and therefore a sampling rate of 50Hz was selected.

2.2.3 Bandwidth

The ECG hardware bandwidth is 0.5 to 100Hz which gives a good quality signal without the excessive baseline wander associated with a full diagnostic bandwidth (0.05 - 100Hz). The low frequency end of the respiration hardware bandwidth had to be as close to DC as was practical so that the signals at low respiration rates were not attenuated significantly. As with the ECG signal, there is a trade off between low end bandwidth and baseline wander. Overall individual respiration channel bandwidth was 0.05 to 25Hz, while the high end of the bandwidth for the multiplexed portions of the circuitry was required to be ten to twenty times higher so as not to cause degradation or mixing of the individual channels.

2.2.4 Isolation and Defibrillation Protection

For the purpose of patient safety, any device that is directly connected to a patient by conductive materials must have its patient connections electrically isolated from A/C line power and earth ground. This requirement is to preclude the possibility of electrical shock by risk currents should the patient come in contact with other non isolated equipment or

earth ground (risk current paths). The Association for the Advancement of Medical Instrumentation (AAMI) publishes specific requirements and specifications for medical equipment relating to patient safety. For patient connected equipment, risk currents must not exceed 10 micro amps between all patient connections and earth ground and between all patient connections and A/C line power. Additionally, patient connected equipment must be protected from defibrillation potentials. This requirement is to protect the equipment from failure and to assure that the full defibrillation energy is delivered to the patient. Because the front end circuitry of the device for this study connects directly to the patient by means of wires and electrodes, the AAMI requirements apply but are not required because the device is for experimental purposes only. Even though not required, the author chose to include the safety requirements in the design as it is of good conscience and practice to do so. The front end circuitry design incorporates industry standard technology including battery power and opto-coupling isolators to achieve the safety requirements. The inputs from patient connections are protected from defibrillation potentials by means of spark gaps and current limiting resistors which clamp high voltage potentials to 90V. Diode clamping is also used to further protect the circuitry by clamping the inputs to the +/- supply rails.

2.2.5 Power

Power for the front end circuitry is from two sources, a 12V 1.0Ah NICd battery and the personal computer's (PC) power supply via the CIO-DAS08 card. The isolated portion of the circuitry was powered by the battery exclusively. This simplified the design by not

having to incorporate or design an expensive DC-DC converter with sufficient isolation between primary and secondary to meet the isolation specifications. The isolated 12V was used directly in some circuits and was used to generate -12V and +/-6.6V for others by the use of linear voltage regulators and charge-pump inverters. By generating the additional voltages from the single battery, the need for multiple batteries was negated and thus improved reliability by minimizing battery maintenance needs. The non-isolated portion of the front end circuitry was powered by the PC's power supply exclusively. Connection to the PC's power supply was available through the interconnecting cables from the CIO-DAS08 card. The +/-12VPC and +5VPC supplies were used directly for the non-isolated circuits and no additional regulation was required. In addition, the PC's +10.0Vref was used as a reference in the pot-type spirometer drive circuit. Battery charging was provided by an external 24VDC wall adapter module (WAM) through a current limiting resistor which provided a semi-constant current at 62mA. For NICd batteries, a constant current charge is desired and if the charge is at a "trickle" charging rate, it may be applied for extended periods of time without damaging the battery. The WAM is only connected to the battery when the power switch is in the CHARGE position. During charge, the front-end circuitry is disconnected in order to maintain isolation, and is therefore not functional.

2.2.6 Data Acquisition Card Interfacing

The CIO-DAS08 data acquisition card was installed in an 8-bit slot of the computer. Connections from the card to the front end is by means of two DB-37 patch cables. The

connectors were configured as both male and female types at both the CIO-DAS08 card and front end in order to provide automatic cable keying. A total of three signal channels were applied to the CIO-DAS08 card for A/D conversion. All three signal channels were bipolar and scaled for a full scale of +/-5V to correspond with the input range of the CIO-DAS08 card. ECG channel gain and scaling is such that a 1volt output corresponds to 1mV relative to input (RTI). The respiration channels provided nominally a 0.5 to 2 VP-P signal to the A/D card. The spirometer output signal was 0-5V logic level transitions. The fourteen digital control signals for the front end circuitry were generated under software control and outputted by the peripheral input output (PIO) feature (8255) of the CIO-DAS08 card. The two digital outputs from the front end circuitry were input to two of the fixed digital inputs of the CIO-DAS08 card since all the PIO ports were configured as outputs. These I/O lines are TTL levels and are connected directly to the non-isolated portion of the front end circuitry.

2.2.7 Circuit Design

The circuitry used in the front-end is industry standard analog type technology, mostly utilizing commonly available integrated circuits and other standard components. The circuitry is divided into two main sections, isolated and non-isolated. In compliance with the isolation specifications, all the circuitry directly connected to electrically conductive patient connections is contained within the isolated section. Because the isolated section is battery powered, where possible, low power devices were chosen and the amount of isolated circuitry was minimized to reduce power consumption.

The amount and type of circuitry required is directly related to the nature of the signals of interest. In this study, the signals of interest are bio-potentials and as such are very small in amplitude, thus requiring sufficient amplification and processing so that they may cross the isolation barrier and be applied to the analog to digital (A/D) converter. An ECG signal for example, has a nominal amplitude of only 1mV on the body. In order to amplify a signal that small to an amplitude of practical size say 1V, amplification of 1000 is required. Gains of that magnitude require very high CMRR so that the signal of interest is not obscured by unwanted noise. For bio-potential signals, the most common source of noise is 60Hz pickup. The human body picks up the 60Hz signal from nearby power lines, lighting and other electrical equipment. This type noise may be several magnitudes higher in amplitude than the signal of interest. Because the noise is distributed across the body, it is seen as common-mode noise to the instrumentation. For a good quality ECG, a CMRR on the order of at least 90dB is desired. The most common method and the method chosen in this design for achieving a high CMRR is the use of an instrumentation amplifier. However, an instrumentation amplifier alone is not sufficient and additional noise canceling techniques are needed. Two methods used in this design are a driven guard and notch filtering. The driven guard is a signal that is composed of the sums of the input signals and is driven by an amplifier through an electrode back onto the body in order to make the noise signal more truly common mode. The notch filter circuit used is an active twin-T type which yields a very deep yet narrow reject band at 60Hz. A downfall of the notch filter is that it rings in response to high frequency transients. Typically circuitry is implemented to suppress pace-maker spikes from causing ringing and

also injecting a pacer marker after the notch filter. Pacer detection and marking is beyond

the scope of this thesis and was not included in the design. The front-end schematic was

drawn using PC based SCHEMA schematic capture software. Copies of the schematics

are provided in appendix 1.

2.3 Front End Theory of Operation

The front end circuitry can be divided into five main sections, the respiration channel, the

ECG channel, the spirometer channel, control logic and power supply. Each section is

divided into subsections or functional blocks. The organization of these functional blocks

is shown in figure 2.3.1. For detailed understanding, refer to the front-end schematic

located in appendix 1 and the theory of operation provided in appendix 2.

2.4 Front-End Construction

After designing the front end schematic using SCHEMA schematic capture software, an

assembly drawing was created using PADS printed circuit board layout software. The

components were arranged on a 0.1" grid for easy transfer perforated proto-board.

Copies of the assembly drawings showing component outlines and reference designators

are provided in appendix 1. Factors affecting component placement included connection

length minimization, feedback paths, isolation spacing requirements and enclosure

dimensions. A 0.1" grid perforated board was cut to drawn dimensions and components

were positioned directly from the assembly drawing. A smaller board was added after

design changes required additional components which would not fit on the main board.
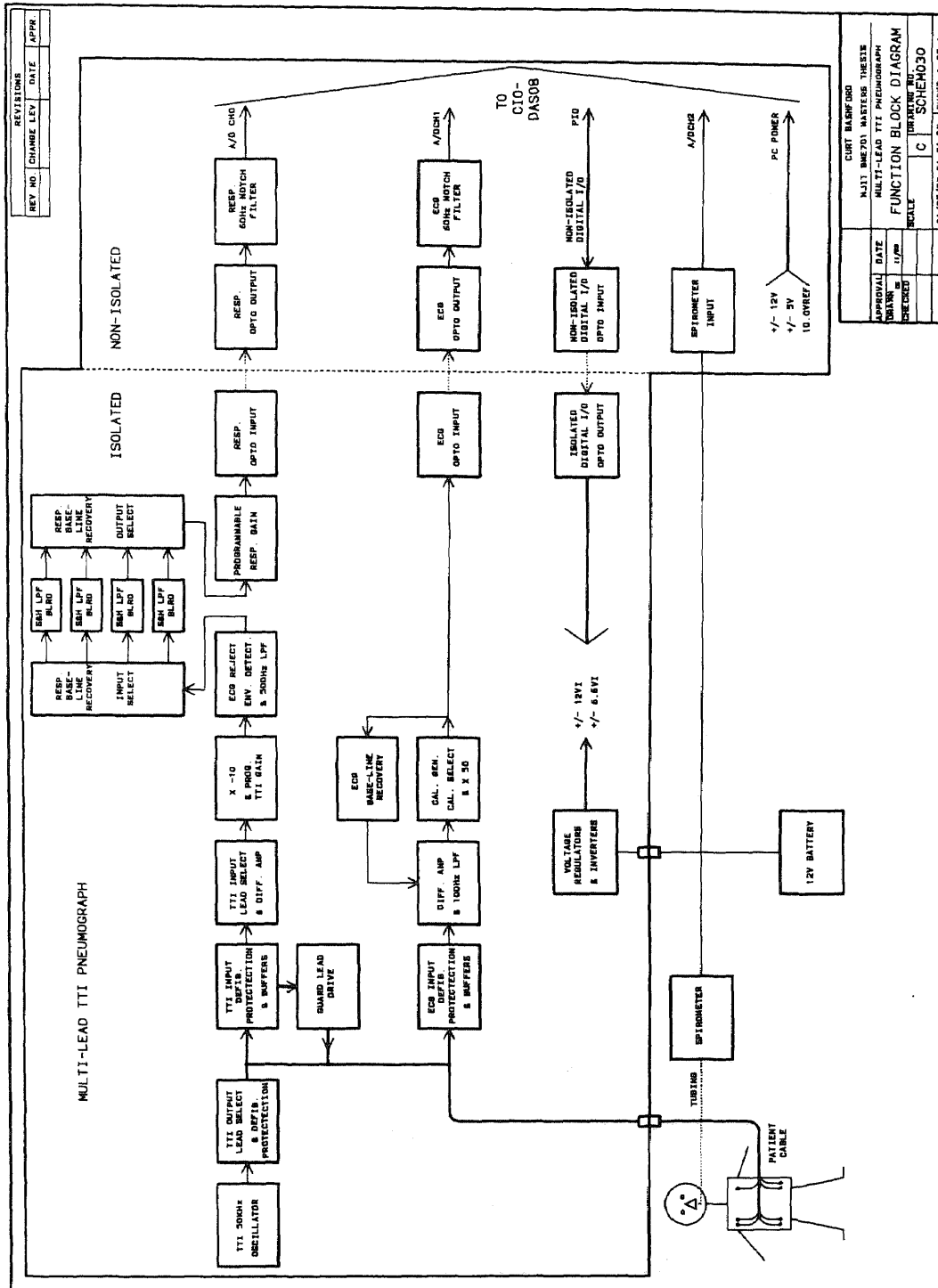
Figure 2.3.1 Front-end function block diagram.

Bifurcated and trifurcated wire wrap pins were installed for most components and DIP sockets were used for integrated circuits. Connections were made using wire wrap techniques because of the large number of components and its advantages for proto-typing. When done correctly, wire wrap provides very reliable connections. This is due to its inherent redundancy since there are typically seven wraps, each of which forms four gas-tight connections for at total of twenty eight connections on average at each pin connection. Three wire colors, red, green, and copper where used to distinguish between power, ground and signal connections respectively.

The circuit boards were mounted in a 3.25H x 10.25W x 7.5D desk top enclosure. Connectors were provided in the enclosure's end panels for connection to external equipment. End panel mechanical drawings and labeling art were created using AutoCAD drafting software. All the front end circuitry is contained within the front end enclosure except for the battery which is connected via a rear panel mounted jack. The jacks for the battery and wall adapter module were chosen as 1.3 and 2.1mm DC power jacks respectively so that their plugs could not be incorrectly connected and break the isolation. The patient cable connector is an AAMI standard 6-pin. Three 3.5mm phono type jacks are provided for connection to the spirometers and event marker. Two BNC jacks are provided for monitoring the ECG and Respiration signals on an oscilloscope. LED indicators are provided to indicate power status labeled BATTERY and COMPUTER. A three position toggle switch for selecting power as ON (battery), OFF and CHARGE is mounted on the rear panel as are the two DB-37 connectors for connection to the CIO-DAS08 card. Copies of the engineering drawing are provided in appendix 1.

2.5 Spirometer

2.5.1 TTL Type

The TTL type spirometer used is a Harvard Instruments Dry-Gas Meter. This device is essentially a standard utility type natural gas meter with a special electronic reader attached to the mechanical meter drive. The gas input and output fittings are modified to fit standard respirator tubing. The spirometer is used in conjunction with a face mask that is fitted with a one-way valve assembly. The one-way valve allows inspired air to enter from one port and exhaled air to exit through another. The gas input is connected by a six foot length of tubing to the expiration port of the valve assembly on the face mask. This configuration ensures that the patient inhales fresh air directly through the inspiration port of the valve assembly and not through the spirometer or tubing as a measure of infection control. This configuration limits the measurements to exhalation volumes only.

The electronic reader of the spirometer displays the total volume on an LCD and is reset to zero with a reset button. The reader also outputs TTL (0 or 5V) levels to a 3.5mm mono jack where each transition corresponds to 0.05L of air expired. The resolution of the spirometer is 0.05L and therefore for each breath there is a +/- 0.05L tolerance in the readings. A software or hardware counter must be used to convert the number of transitions into volume readings. During inspiration or pauses in breathing no air passes through the spirometer and therefore the output does not change level and remains at the previous logic state. For this study, the output of the spirometer was connected to the TTL SPIROMETER jack of the front-end with a 3.5mm mono patch cable.

2.5.2 Potentiometer Type

A second type spirometer, a potentiometer type, was considered for use. This spirometer is mechanically coupled to the shaft of a continuous rotation potentiometer with contacts which are available for connection to external equipment. One complete revolution of the potentiometer corresponds to 10L of air expired. This type spirometer uses the same mask/valve assembly used with the TTL type spirometer. To measure volumes, a stable voltage source is applied to one of the leg terminals of the potentiometer and ground to the other leg. The voltage measured at the wiper terminal of the potentiometer corresponds to the volume of air expired. In order to determine the volume expired for each breath, the voltage difference between the start and end of expiration has to be measured or calculated with consideration for rotation of the potentiometer past 360 degrees since the voltage goes from full scale to zero.

The front-end provided a 3.5mm stereo jack for connection to the potentiometer. The voltage supply provided at this jack is a precision 5.0VDC which yields a scale factor of 1V = 2L since the full scale range will be 5V corresponding to one rotation which corresponds to 10L. The resolution of this device is limited only to the resolution of the potentiometer which is high since it is a precision type wire-wound potentiometer. There is also a portion of the rotation at the transition near 360 degrees where the output is open circuit and accurate readings may not be possible if expiration starts or ends in this region. Although accommodated for, this spirometer was not used because it was taken out of service for repair prior to performing the clinical trials for this study.

2.6 Data Acquisition Card

The data acquisition card selected is CIO-DAS08 manufactured by Computer Boards INC. of Mansfield, Ma. The CIO-DAS08 is a multifunction analog and digital I/O card designed to be compatible with MetraByte's DAS08. The CIO-DAS08 also features a PIO-12 compatible 8255 and 37 pin connector which provides 24 programmable TTL I/O lines in addition to the 3 fixed digital inputs and 4 digital outputs. The on board Analog to Digital (A/D) converter is an industry standard 574 with 12 bit resolution connected to a multiplexor that provides 8 single ended channels with a 2uSec. sample and hold. Input ranges are DIP switch selectable as +/-5V, +/-10V or 0-10V. An on board 8254 provides 33 16 bit counter/timers. Connection to the front-end is provided by 2 DB37 connectors 1 male and 1 female for keying along with 6' patch cables. The CIO-DAS08 can be controlled by programs in BASIC, C, FORTRAN or PASCAL, for this application the C language was used. In order to simplify programming the "Universal Library" software was purchased with the board so that canned functions could be used where possible. Refer to the schematics in appendix 1 for connection information and pin-outs for the CIO-DAS08 card's connectors.

2.7 Computer

The computer used for all the Computer Aided Drafting, data acquisition, signal processing and data analysis is an AT type Personal Computer with a 486-33DX CPU, VESA local-bus, 256K Cashe, 8M RAM, 250M hard drive and dual floppies. The CIO-DAS08 acquisition card was installed on an 8-bit card slot with it's base address at 300H.

The data acquisition program runs under DOS while the signal processing and data analysis was performed using MATLAB and S-Plus software which run under Windows 3.1. No additional computer hardware was required, although the signal processing would run faster with additional RAM.

CHAPTER 3

METHODS

3.1 Overview

In order to determine respiratory tidal volume by trans-thoracic impedance pneumography, data were acquired by using both hardware and software designed specifically for this thesis. Acquired data included 4 channels (leads I, II, III and IV) of respiration, a spirometer channel, and 1 channel of ECG (lead II). The respiration data were acquired as 4 time-division multiplexed channels. The respiration signal was acquired by biploar trans-thoracic impedance pneumography. It was bipolar because the oscillator signal input was applied to the same 2 electrodes as the signal was measured from. The multiplexing allows 4 separate channels or leads to be simultaneously acquired onto 1 A/D channel. By having 4 leads of respiration, measurements from 4 different positions on the body were provided so that the data may be combined such that respiratory tidal volume may be determined with accuracy and consistency that is superior to that of single lead impedance pneumography. The ECG channel data provides a lead II ECG for direct use in heart-rate variability studies. It would advantageous to obtain the ECG from the RA-LL pair of respiration electrodes since it would eliminate two electrodes and lead wires that connect to the subject. Unfortunately it was determined in testing that this method is not possible because the as the impedance signal is switched in and out of the electrodes, changing offsets result in noise which totally obscures the ECG

37

signal. The spirometer data is used for determining the accuracy of the impedance based tidal volume calculations and ultimately for calibration of the impedance measurement.

Data were collected from a total of 6 subjects, 3 males and 3 females, varying in age from 28 to 38. This chapter discuses the methods used in conjunction with the equipment described in chapter 2. Methods of clinical trial protocol, data acquisition and signal processing are discussed in detail.

3.2 Clinical Trial Protocol

In preparation for testing the subjects were briefed on the test protocol and equipment to which they were to be connected and were assured of its safety and cleanliness to reduce possible anxiety. A standardized protocol for acquiring data was used for each subject.

Setup involved affixing the electrodes to the subject. Standard ECG silver-silver-chloride electrodes, 3M Red Dot type were used. Electrode placement sites were prepped by abrading the skin with a scratcher and cleaning with alcohol wipes as recommended by Smith [14]. A total of 7 electrodes were used, 4 for respiration, 2 for ECG and 1 for guarding for. Electrodes were placed on the subject as shown in figure 3.2.1. Respiration electrodes (RA, LA, LL and RL) were placed in the standard ECG chest locations. Right Arm (RA) and Left Arm (LA) electrodes were placed on the right and left anterior respectively at the first intercostal space just below the clavicles. The Right Leg (RL) and Left Leg (LL) electrodes were placed laterally over the last intercostal space on the right and left respectively. The guard electrode was placed just posterior to the RL electrode. The two ECG electrodes (ECG-RA and ECG-LL) were placed in the standard ECG Lead

II configuration adjacent to the respiration RA and LL electrodes. The respective patient cable lead wires were connected to the electrodes and the patient cable plugged into the front-end.
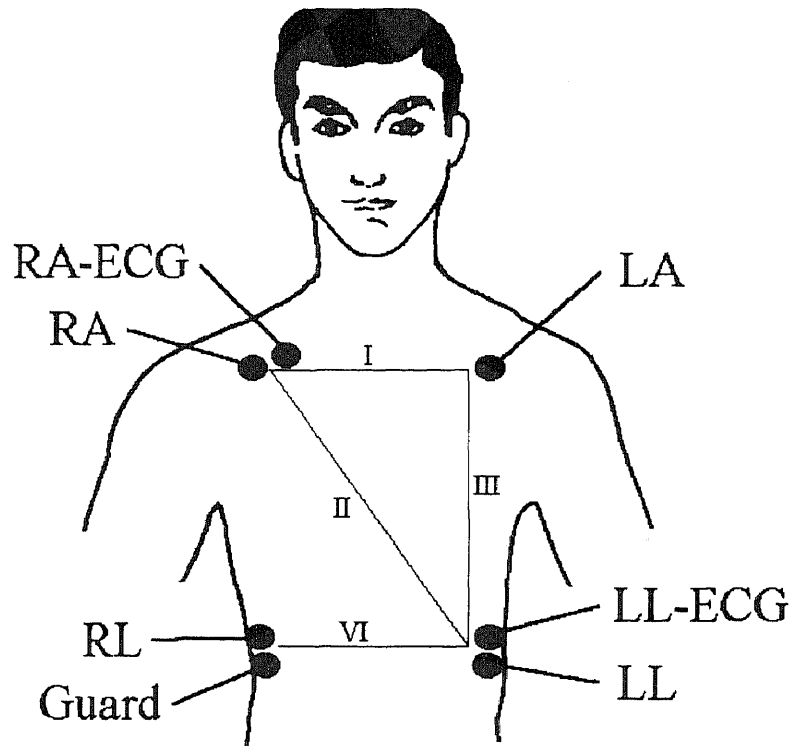
Figure 3.2.1 Electrode placement locations used.

The face mask was positioned over the subject's mouth and nose and secured in place with the cap and Velcro straps. Tension was adjusted so the that air did not leak from the sides of the mask. The spirometer tubing was connected to the mask and the spirometer output connected to the front-end with the patch cable.

With the subject in a seated position, the acquisition program was run for several seconds so that the data displayed could be checked to assure proper setup. When ready,

the actual trials were begun by re-starting the acquisition program. The protocol included 5 - 90 second trials for each subject for a total of 30 trials. The 5 trials included one random (non-paced) breathing, 1 paced breathing at 8 breaths per minute (BPM, not to be confused with beats per minute referring to heart rate), 1 paced breathing at 12 BPM, 1 paced breathing at 18 BPM and 1 combination paced breathing at 30 seconds each of 8, 12 and 18 BPM. Paced breathing was accomplished by having the subject synchronize his/her breathing with the LEDs on a custom pacing device. This device sequenced a series of dual color LEDs from one end to the other and back at the selected rate. The LEDs alternate color between red and green for each direction of the sequencing. The subject was instructed to synchronize his/her breathing such that inspiration coincided with the green phase and expiration with the red phase.

After running a trial, a data file containing raw ASCII data for the 4 respiration leads, ECG lead II and spirometer output was created and saved for each trial.

3.3 Data Acquisition

3.3.1 General

The trial data was acquired by the front-end and the CIO-DAS08 card under control of the ACQUIRE.EXE acquisition program. This program was written in the "C" programming language. The acquisition program controls the front-end by use of the programmable digital I/O provided on the CIO-DAS08 card. Functions of the acquire program include control of respiration lead selection and multiplexing, gain control, A/D

channel control and data conversion, graphical display of data waveforms and file storage of 6 channels of acquired data arranged as columns in ASCII format..

3.3.2 Running the Acquire Program

The ACQUIRE.EXE program runs under DOS and is executed by typing "ACQUIRE" at the prompt. Once started, the operator is prompted to wait at least 15 seconds before pressing any key to start the acquisition. This delay allows time for the data array to be cleared to zeros and for the signal baselines to settle. An oscilloscope can be connected to the BNC outputs if desired to view the signals before beginning the acquisition. After starting the acquisition the display prompts the operator that the program is acquiring and that pressing any key will cancel the acquisition. When the acquisition is completed or canceled, the acquired signal waveforms are displayed and advanced one screen at a time by pressing Enter. The display sequence is 8 screens of ECG, then 2 screens of Spirometer followed by 1 screen each of respiration leads Resp 1 to Resp 4. After all the waveforms have been displayed the operator is prompted to respond Yes or No to save the data to a file named TRIALX.DAT. The program has now completed and the saved file can be renamed to a different name (usually replacing the X with the trial number).

3.3.3 Acquire Program Theory of Operation

Refer to the block diagram of figure 3.3.1 and the ACQUIRE.CPP program source code listing located in appendix 3 to aid in understanding the following detailed description of the operation of the ACQUIRE program.

The first section of the program sets the "include" function libraries and declares and initializes the variables. The variable "MAXSAMPLE" is the maximum number of samples for the respiration lead variables Resp1 to Resp4. The number of samples for spirometer data "Spiro" is 2 x MAXSAMPLE since it is at twice the sampling rate of the Resp data. Likewise ECG is 8 x MAXSAMPLE since it is at 8 times the sampling rate of the Resp data. The largest number allowed for MAXSAMPLE is limited to what will compile and link for the array size used and is approximately 2300. A MAXSAMPLE of 2250 was chosen which gives a run time of 90 second since,

$$\text{Runtime} = \text{MAXSAMPLE} \times \frac{1}{\text{Resp sample rate}} \qquad \text{(Eq. 3.1)}$$

$$\text{Runtime} = 2250 \times \frac{1}{25 Hz} = 90 \text{ sec.} \qquad \text{(Eq. 3.2)}$$

The next section in the program defines the function prototypes, which are functions that will be called by the main loop. The "Sdelay" function is a short delay loop which is a simple incrementing "for" loop used by the ADCIn function. The "ADCIn" is the routine for reading a single sample by the A/D converter. It sets the CIO-DAS08's multiplexer channel (to 1 of 8), starts a 12 bit conversion, waits for end of conversion and scales and outputs the data. The "plot" function has separate routines for displaying the acquired data on the screen for each of the 6 channels using graphics mode. The waveforms are displayed as cascading from top left to bottom right and multiple screens are used for Spiro and ECG since they are sampled at higher rates than the Resp data.
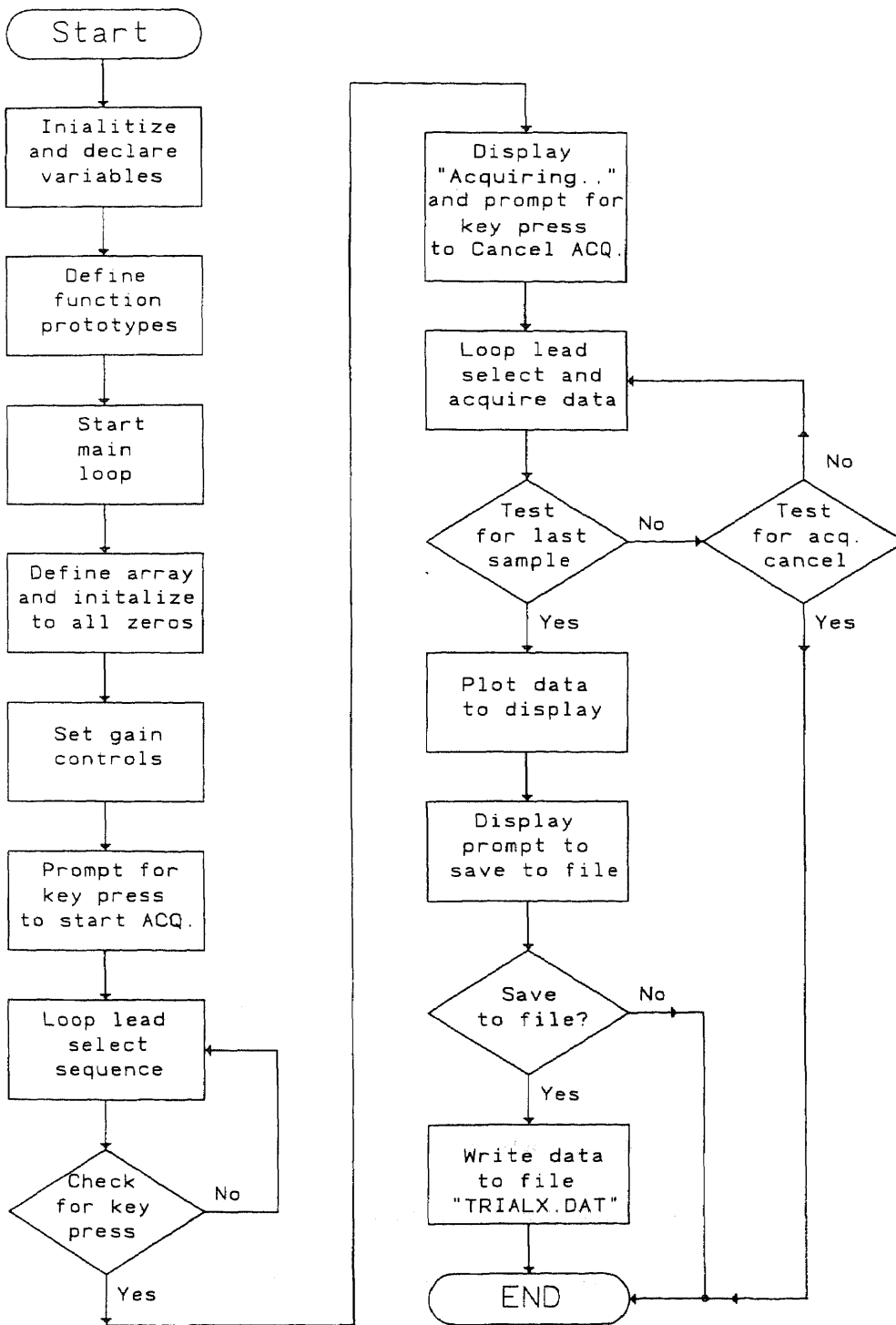
Figure 3.3.1 Flow chart for the ACQUIRE program.

The main loop of the program begins by declaring the pointers for each of the 6 channels of data and setting all the data in the array to zero. The next section sets the gain control outputs by writing to the 8255 of the CIO-DAS08 card with the cbDOut command. Next the first set of prompts are written to the display by the "printf" statements. The program then scans for a key press before jumping to the acquisition routine. While it is scanning, a lead selection routine is running to activate the front end circuitry and stabilize the baseline. The lead selection sequence is critical to define the sampling rates and to suppress switching transients that occur with lead selection. The sequence is as follows:

1) Set the lead select to lead I and switch the baseline select switch to disabled.

2) Wait 3 mS to allow the switching transient to pass.

3) Enable the baseline select switch.

4) Wait 7mS, the period of valid data.

5) Switch the baseline select switch to disabled.

6) Go to the next case

7) Select the next lead (i.e. lead II).

8) Repeat the above steps for each of the 4 leads and loop.

Once a key is pressed, the acquisition routine is started. The "Acquiring data !" prompt is written to the display and the keyboard is again scanned for a key press to cancel the acquisition routine. During acquisition a lead selection sequence similar to the one during acquisition start is looped. In addition to lead selection, A/D conversions are called and the data is acquired. The acquisition sequence is as follows (case 0):

1) Read the spirometer channel with the A/D and increment its pointer.

2) Set the lead select to lead I and switch the baseline select switch to disabled.

3) Wait 3 mS to allow the switching transient to pass.

4) Enable the baseline select switch.

5) Wait 2 mS for sampling timing.

6) Read the ECG channel with the A/D and increment its pointer.

7) Wait 2 mS for to be in the center of the valid Resp data period.

8) Read the Resp1 channel with the A/D and increment its pointer.

9) Wait 3 mS for sampling timing.

10) Read the ECG channel again with the A/D and increment its pointer.

11) Switch the baseline select switch to disabled.

The above sequence is repeated for cases 1, 2, and 3 with the exception that the spirometer channel is only read during case 0 and case 2. It can be seen that the processing time for each case is the sum of the delays which is 10mS since execution time is negligible. Since there are four cases the total processing time for one complete loop is 40mS. The sampling rates can be determined knowing that in one complete loop;

- The Spirometer channel is sampled twice, once every 20mS or at 50Hz.

- The Resp channels are sampled once each, once every 40mS or at 25Hz.

- The ECG channel is sampled 4 times, once every 5mS or at 200Hz.

The acquisition loop is repeated until the number of passes equals MAXSAMPLE (2250) or a key is pressed to cancel the acquisition. When the acquisition loop is exited the "plot" function is called and the waveforms are displayed on the screen. After the operator pages through the waveforms by pressing any key, the "Save data to file: TRIALX.DAT ? [Y/N]" prompt is written to the display. The Y and N keys are then scanned. If a N is pressed (no save), no action is taken and the program exits. If the Y key is pressed (save data), a file named "TRIALX.DAT" is opened and the data is written as ASCII in columns defined by the fprintf statements.

The first line of the file contains the value of MAXSAMPLE in the first column and zeros in each of the other 13 columns. This automatically provides the number of data samples per column for post processing analysis programs. The remaining lines of the file contain the acquired data in 14 columns where:

- Columns 1 and 2 = Spiro data (alternating).

- Column 3 = Resp1 data.

- Column 4 = Resp2 data.

- Column 5 = Resp3 data.

- Column 6 = Resp4 data.

- Columns 7 through 14 = ECG data (alternating).

3.4 Signal Processing

3.4.1 General

Once acquired and stored in files, the signal data is processed using programs written for use with MATLAB software. The raw acquired data is not in a directly useable format. The desired information is buried within the raw data and needs to be extracted. The purpose of the signal processing programs is to process the raw acquired data into a form from which it can be used and to extract the desired information. This information can then be applied to the data analysis programs. Because the spirometer that was used supplies only expiration volume data, it is not possible to properly evaluate inspiration data. The following signal processing programs function under the premise that respiratory tidal volume for a particular breath is directly related to the difference in signal amplitude from the start of expiration to the end of expiration for that breath. Refer to the MATLAB program listings located in appendix 3, to aid in understanding the following detailed descriptions of the signal processing programs.

3.4.2 RUNTRIAL Program

The RUNTRIAL program is the master "batch" program. It serves to simplify and automate the MATLAB signal processing programs. The first operation of RUNTRIAL loads the raw ASCII trial data from a file named TRIAL**.dat (** = the trial #.). Once loaded, batch programs for the three signal types are executed; SPRUN which processes spirometer data, IPRUN which processes impedance pneumograph data and ECGRUN, which processes ECG data. After these programs have run, the new data is saved for

future use. The flow chart for the RUNTRIAL program is shown in figure 3.4.1 and the

individual batch programs are discussed in detail in the following sections.

```
┌─────────────────────────┐
│         START           │
└─────────────────────────┘
            │
┌─────────────────────────┐
│  Load data from ASCII   │
│    TRIALX.DAT file      │
└─────────────────────────┘
            │
┌─────────────────────────┐
│     CALL SPRUN.M        │
│     Process the         │
│    spirometer data      │
└─────────────────────────┘
            │
┌─────────────────────────┐
│     CALL IPRUN.M        │
│     Process the         │
│       IP data           │
└─────────────────────────┘
            │
┌─────────────────────────┐
│     CALL ECGRUN.M       │
│     Process the         │
│      ECG data           │
└─────────────────────────┘
            │
┌─────────────────────────┐
│      Save results       │
└─────────────────────────┘
            │
┌─────────────────────────┐
│          END            │
└─────────────────────────┘
```
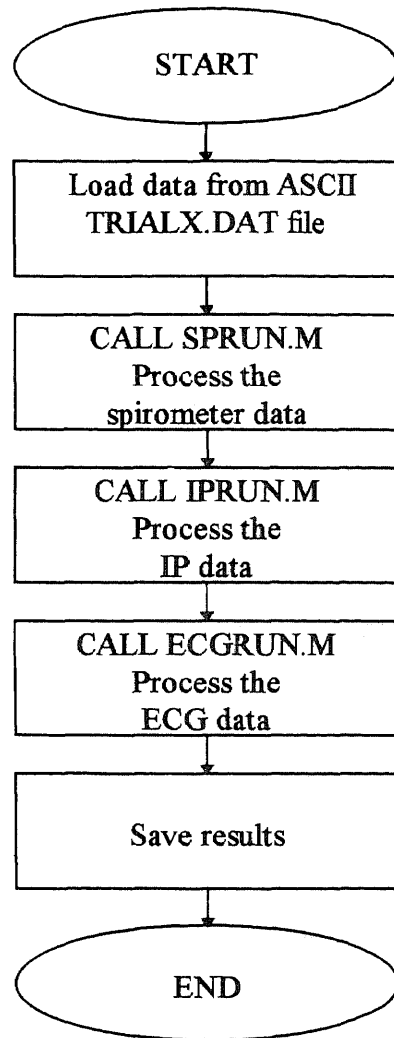
Figure 3.4.1 Flow chart for RUNTRIAL program.

3.4.3 SPRUN Programs

The program SPRUN is the batch program called by RUNTRIAL to execute the spirometer signal processing programs. Its only function, as shown by the flow chart of figure 3.4.2, is to call the programs SPLOAD, SPRANGE, SPINDEX, and SPVOL.

The first function of SPRUN is to call the program SPLOAD. SPLOAD first loads the number of samples stored in the data at row 1 col.1 "MAXSAMPLE"). It next loads the spirometer data as SPIRO from columns 1 and 2 by alternating them until MAXSAMPLE is reached. The SPIRO data is initially scaled to correspond to +/-5V, and is then compared to a threshold of 2 and scaled as a 1 or 0. Figure 3.4.3 shows a sample of the scaled spirometer data plotted against the index.

The next program called by SPRUN is SPRANGE. SPRANGE determines the ranges of inspiration (0) and expiration (1) from the SPIRO data. It does this by testing for transitions within the SPIRO data since the spirometer generates transitions every 0.05L during expiration and none during inspiration. The program looks ahead over the next 1 sec. of data as it tests for transitions between inspiration and expiration in order to distinguish between a slow expiration and the true end of expiration. An envelope of the spirometer data is generated where periods of inspiration are "0" and periods of expiration are "1", a sample of which is shown in figure 3.4.4.

Once the spirometer ranges of inspiration and expiration are determined, the SPINDEX program determines and stores the number of valid breaths (totalnb) and the inspiration and expiration starting and ending indexes. For a breath to be valid, it must be a complete cycle with both a start of inspiration and end of expiration.
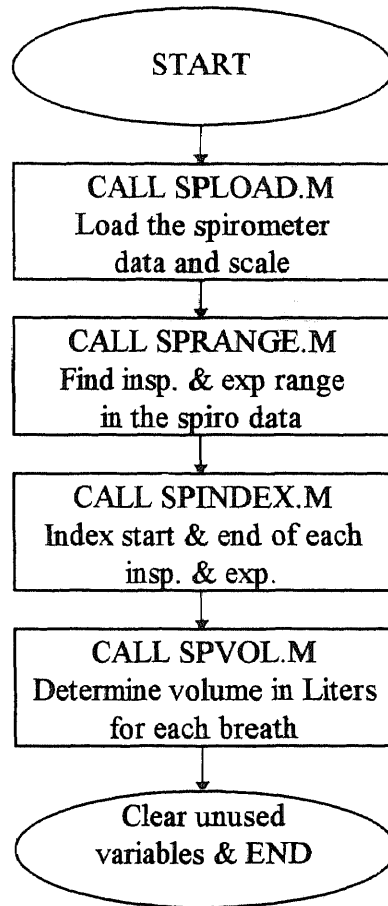
Figure 3.4.2 Flow chart for SPRUN program.

The last program called by SPRUN is SPVOL. SPVOL determines the spirometer volume for each breath using the indexes determined by SPINDEX. It accomplishes this by counting the number of transitions in the indexed expiration range (spexstart to spexend) and multiplying by 0.05 since each spirometer transition corresponds to 0.05L of air expired. The calculated spirometer volumes are saved as SPVOL. A sample plot of SPVOL data is shown in figure 3.4.5.
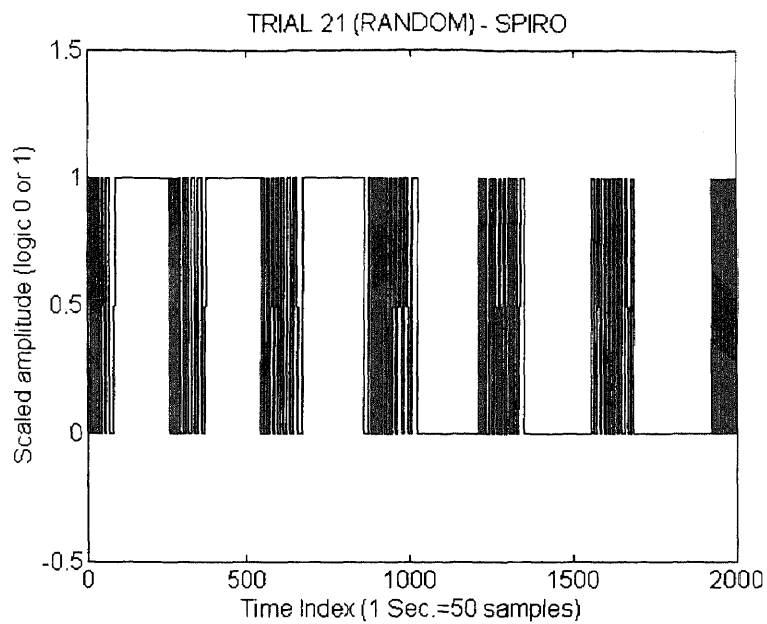
Figure 3.4.3 Sample plot of scaled spirometer transition data plotted against the index.
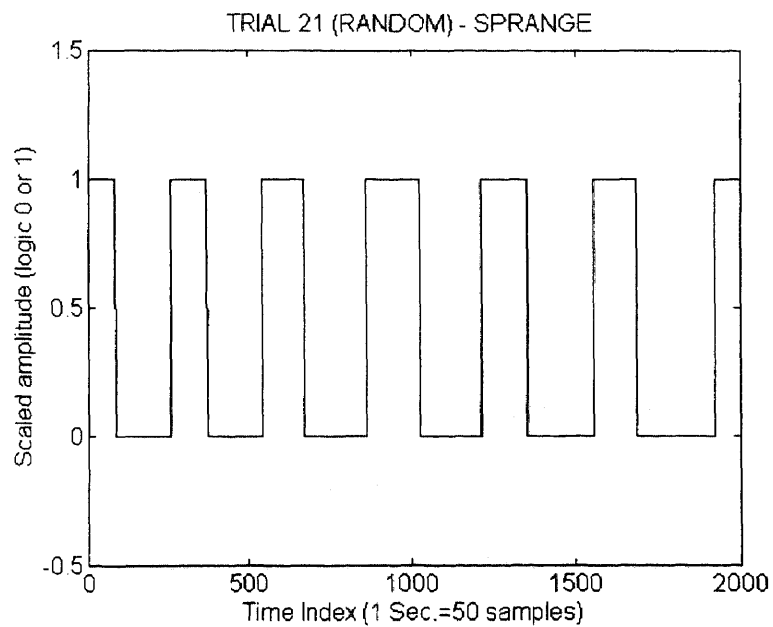
Figure 3.4.4 Sample plot of SPRANGE Vs. index, an envelope of the spirometer data.

TRIAL 21 (RANDOM) - SPVOL
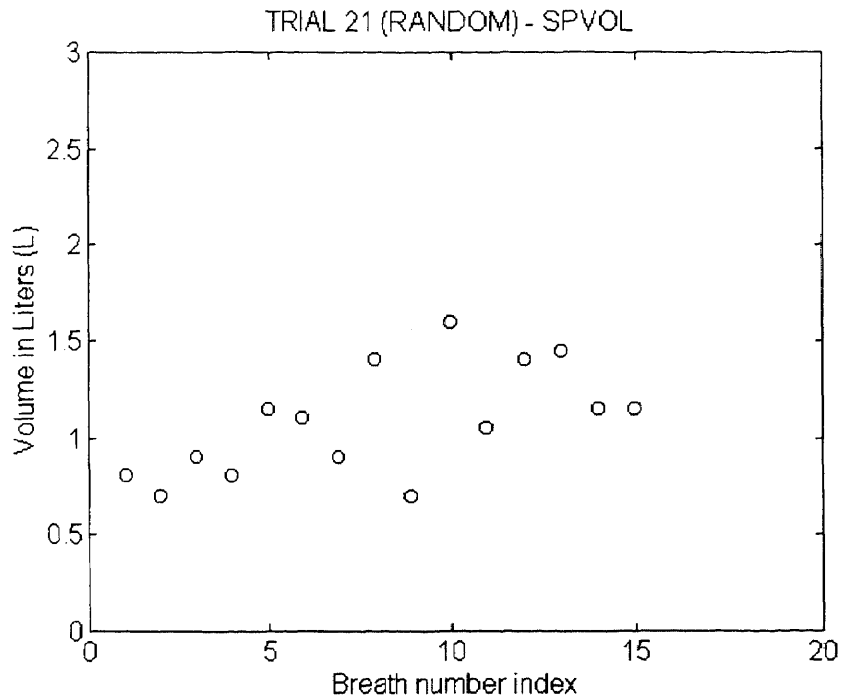
Figure 3.4.5 Sample plot of SPVOL data, amplitude in (L) Vs. breath number index.

3.4.4 IPRUN Programs

The program IPRUN is the batch program called by RUNTRIAL to execute the impedance pneumograph signal processing programs. As shown in the flow chart of figure 3.4.6, its only function is to call the programs IPLOAD, IPINTREP, IPFILT, IPINDEX, and IPDIFF.

The first function of IPRUN is to call the program IPLOAD. IPLOAD first loads the number of samples stored in the data at row 1 col.1 "MAXSAMPLE"). It next loads the 4 sets (leads) of respiration data as IP1 to IP4 from columns 3,4,5 and 6 respectfully, until MAXSAMPLE is reached. Each lead of the IP data is scaled in amplitude to correspond to +/-5V.
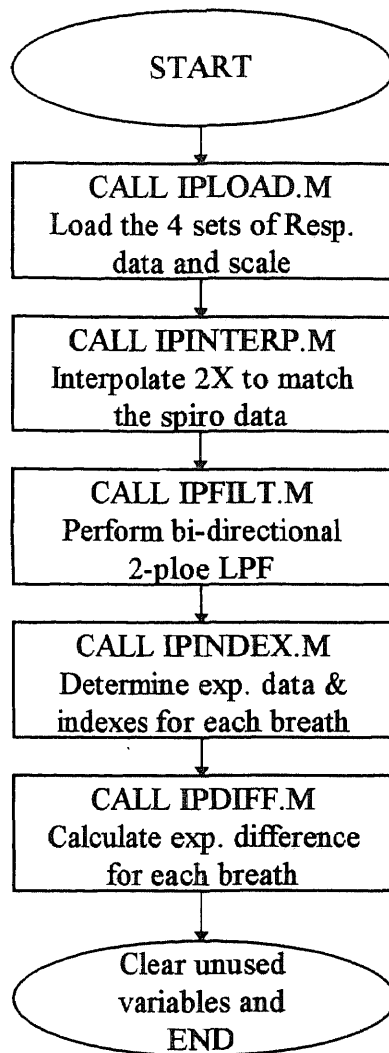
Figure 3.4.6 Flow chart for IPRUN program.

The respiration data is sampled at 25 Hz, while the spirometer data is sampled at 50 Hz. In order to simplify the signal processing, a linear interpolation routine in MATLAB is applied to the respiration (IP) data so that the amount of data samples is doubled in order to match the amount of spirometer data samples. The program IPINTERP performs this function for each of the 4 sets of IP data. The scaled IP data is noisy and needs to be filtered to remove high frequency noise introduced during

acquisition. The next program, IPFILT, filters each of the IP data with a 2-pole bi-directional low pass filter with Fc=6.25 Hz. The bi-direction is required to cancel time domain phase shift that occurs with the software filtering. The MATLAB function "filtfilt" performs this function automatically. Sample plots of unfiltered and filtered IP data Vs. their index are shown in figures 3.4.7 and 3.4.8 respectively.

Once the IP data is filtered, program IPINDEX is run. IPINDEX is similar to SPINDEX in that it determines the start and end indexes for the inspiration and expiration of each breath. The peaks and valleys (maximum and minimum) of the IP signal correspond to transitions between inspiration and expiration. IPINDEX uses the indexes determined by SPINDEX as a range in which to test for a minimum or maximum. The slope of the IP signal is first tested to determine if it is polarity inverted, in which case a maximum instead of a minimum indicates the start of an inspiration. The converse is true
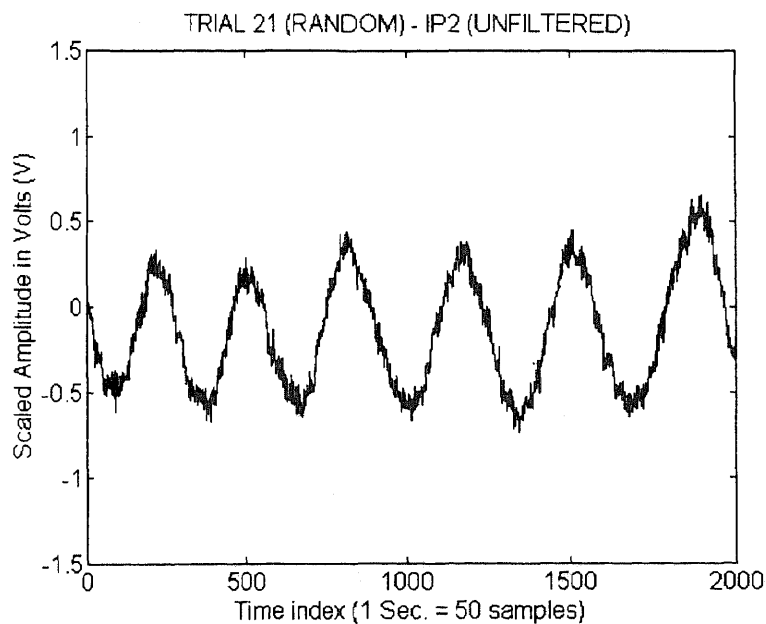
Figure 3.4.7 Sample plot of unfiltered IP data.

TRIAL 21 (RANDOM) - IP2 (FILTERED)
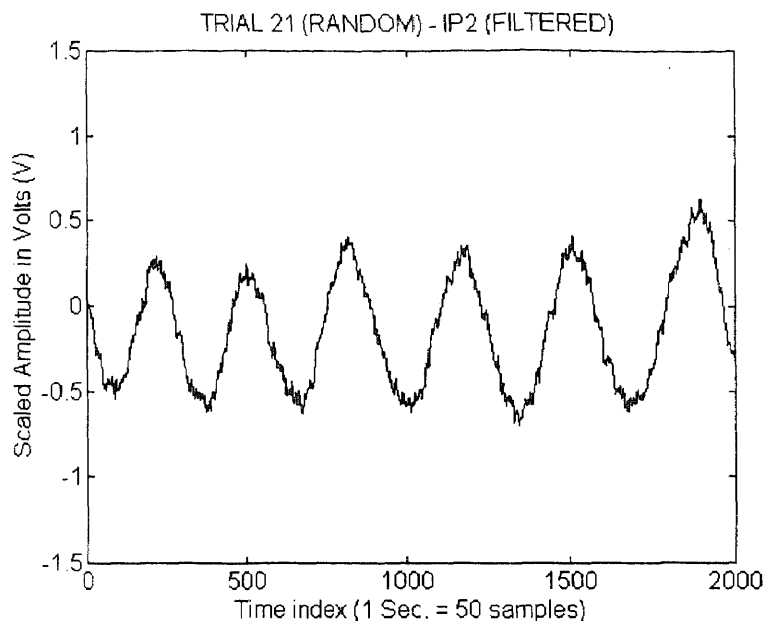
Figure 3.4.8 Sample plot of filtered IP data.

for the start of expiration. This process is performed for each valid breath (as determined by SPINDEX) for each lead of IPdata (IP1 - IP4). The plot of figure 3.4.9 shows one lead of IP data (IP1) plotted with the corresponding SPRANGE data for the same index. From the plot it can be observed that there is a time lag between the IP lead data and the SPRANGE spirometer data that must be accommodated for when determining the peaks and valleys of the IP signals.

The last program called by IPRUN is IPDIFF. IPDIFF calculates the amplitude difference between the maximum and minimum for each breath of each lead of IP using the data determined by IPINDEX. The generated data, IP1DIFF, IP2DIFF, IP3DIFF and IP4DIFF are the impedance pneumograph (difference) volumes that will be used in the data analysis.
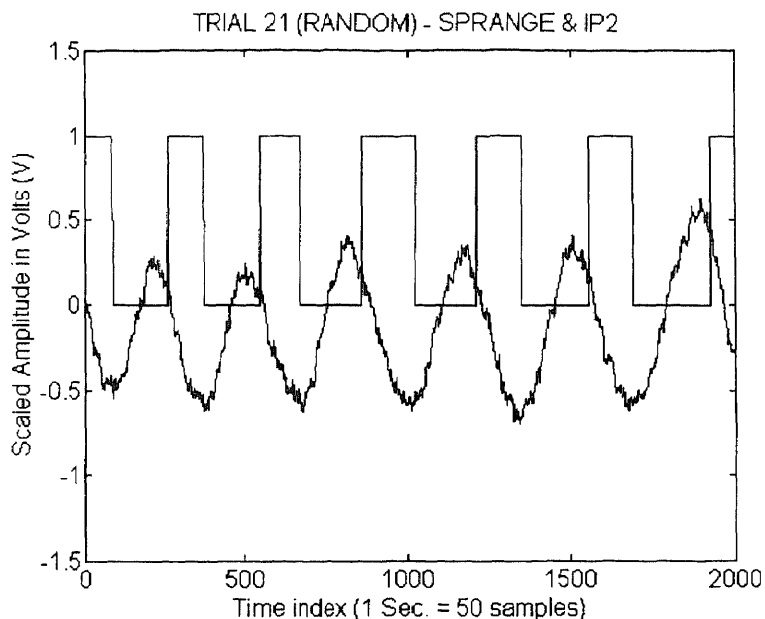
Figure 3.4.9 Sample plot of an IP lead signal overlaid onto the corresponding SPRANGE data, showing the time lag between the two.

3.4.5 ECGRUN Programs

The program ECGRUN is the batch program called by RUNTRIAL to execute the ECG signal processing programs. As shown in the flow chart of figure 3.4.10, its only function is to call the programs ECGLOAD and ECGFILT.

The ECG data is processed only for noise removal and scaling to determine if it is adequate so that it may be available for future processing. The program ECGLOAD, first loads the number of samples stored in the data at row 1 col.1 "MAXSAMPLE"). It next loads the ECG data from columns 7 through 14 by alternating columns until MAXSAMPLE is reached. The ECG data is scaled to correspond to +/-5V. It should be noted that the time scale index is 4X the time scale for SP and IP data because the sampling rate is 4X greater.

```
        ┌─────────────────────┐
        │        START        │
        └─────────────────────┘
                   │
                   ▼
        ┌─────────────────────┐
        │   CALL ECGLOAD.M    │
        │  Load ECG data from 8│
        │  columns and scale  │
        └─────────────────────┘
                   │
                   ▼
        ┌─────────────────────┐
        │   CALL ECGFILT.M    │
        │  Perform bi-directional│
        │     2-ploe LPF      │
        └─────────────────────┘
                   │
                   ▼
        ┌─────────────────────┐
        │         END         │
        └─────────────────────┘
```
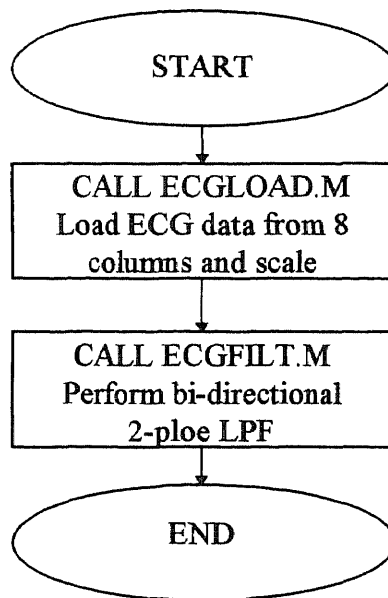
Figure 3.4.10 Flow chart for ECGRUN program.

The scaled ECG data is noisy and requires filtering to remove high frequency noise introduced during acquisition. The program, ECGFILT, filters each of the ECG data with a 2-pole bi-directional low pass filter with Fc=50 Hz. As with the IP data, the bi-direction is required to cancel time domain phase shift that occurs with the software filtering. A sample plot of an actual acquired in trial 16 ECG is shown in figure 3.4.11.

3.5 Data Analysis

3.5.1 General

The results of the signal processing programs provides two sets of data for analysis. These are the spirometer volumes (SPVOL) and the impedance pneumograph peak-valley differences (IP1DIFF, IP2DIFF, IP3DIFF and IP4DIFF). In order to determine how well

the IPDIFF data relates to the SPVOL data, different methods of analysis were performed. These methods involved correlation and modeling of the IPDIFF data vs the SPVOL data.

TRIAL 16 - ECG
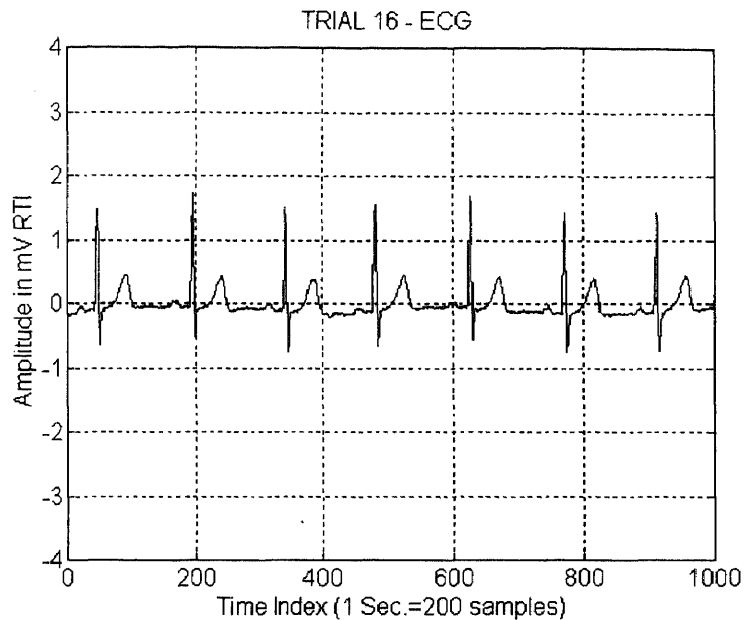
Figure 3.4.11 Sample plot of an actual acquired ECG, amplitude in milliVolts (mV) relative to input (RTI) Vs. index of samples.

3.5.2 Correlation

Correlation coefficients were generated using MATLAB for comparison of the SPVOL data (accepted) with the IPDIFF data (unknown). A correlation coefficient is a dimensionless number that measures the strength of the linear association between two variables. The correlation coefficient (r) is equal to covariance divided by the product of the estimated sample populations.

$$r = Covariance/product\ of\ estimated\ sample\ populations \qquad (Eq.\ 3.3)$$

Covariance (*cov*) is a measure of how two random variables vary together either in a sample or in the population, when the values of the two random variables occur in pairs[13]. If $C = cov(x)$ then $r(x)$ is the matrix whose element (i,j) is:

$$r(i,j) = \frac{C(i,j)}{\sqrt{C(i,j)C(j,i)}}$$ (Eq. 3.4)

A correlation coefficient of 1 indicates that all the points lie on a straight line with positive slope, and a -1 indicates a negative slope.

In MATLAB, the function;

corrcoef(x,y)

is used to determine the correlation coefficients between functions x and y. For this study, x is the SPVOL data and y is the IPDIFF data.

3.5.3 Modeling

In order to perform modeling on the data, the S-Plus for windows version 3.1 software package was used. S-Plus is both a language and an interactive programming environment for data analysis and graphics. Two modeling functions that are available in S-Plus were used to attempt to combine the different leads of impedance volume data (IPDIFF) in such a way that the result might provide a good correlation to the spirometer (SPVOL) data. The functions chosen were the generalized additive model (GAM) and the generalized linear model (GLM).

The GAM uses an adaptive approach to model the terms nonparametrically using a scatter plot smoother. In S-Plus, the output of the GAM function gives numbers for degree of freedom, residuals and the residual deviances. The degree of freedom represents the total number of data points. The residual represents the difference between the actual and simulated data and the residual deviance is the summation of the square of the residuals. The value of the residual deviance determines how good a fit the model is. The smaller the deviances, the better the model. The output of the GAM can estimate the coefficients, evaluate and examine the fits. In particular, the estimated residual and partial residual plots can be used to illustrate discrepant observations and to identify nonlinearities.

The general form of the GAM is as follows:

$$n(x) = f1(x1) + f2(x2) + \ldots + fp(xp) \qquad \text{(Eq. 3.5)}$$

where xi and fi (i=1,2,3...p) are the predictors and the transform functions of the predictors respectively. In this study four transform functions were used with the GAM, no transform, "poly", "s" and lo. The "poly function is a smoothing transform which generates a basis of polynomial regression. The "s" function is a smoothing transform that uses the spline method. The "lo" function is a scatter-plot smoothing transform and uses the robust locally linear fit. The generalized linear model (GLM) is another modeling function supported by S-Plus. It functions similarly to GAM except the model is fit using iterative reweighted least squares (IRLS).

In addition to the default output provided by GAM or GLM, there are "extractor" functions available in S-Plus for extracting additional data. The extractor "coefficients" extracts the transfer function coefficients for each predictor function. The "fitted" extractor extracts the fitted model data, and "residuals" extracts the residuals. The usage of the extractors is of the form:

coefficients(object)

residuals(object)

fitted(object)

Modeling (both GAM and GLM) was performed on the IPDIFF (impedance peak to valley difference) data in order to fit it to the spirometer data (SPVOL). Models were evaluated for each of the transform functions (s, poly and lo) and also with no transform in order to determine which provided the best fit. In addition, several combinations of the IPDIFF data were tested; each lead independently, leads I and II, leads I, II and III, leads I, II, III and IV and lead I and IV. This was done in order to determine what leads or combinations of leads provided the best fit. The direct results of the modeling are presented in numerical form, specifically as residual deviances. To view the results graphically, the fitted model must be extracted. Extracted fitted data can be plotted against SPVOL to graphically see how well the data fits since for an exact fit the data will be aligned in a straight line. Figures 3.5.1 and 3.5.2 show sample plots of GAM and GLM fitted data using the lo transform function for the combination of all leads (IPDIFF of leads I,II,III and IV) respectively. It is apparent from the plots that for the case shown, GAM provided a much better fit than did GLM.
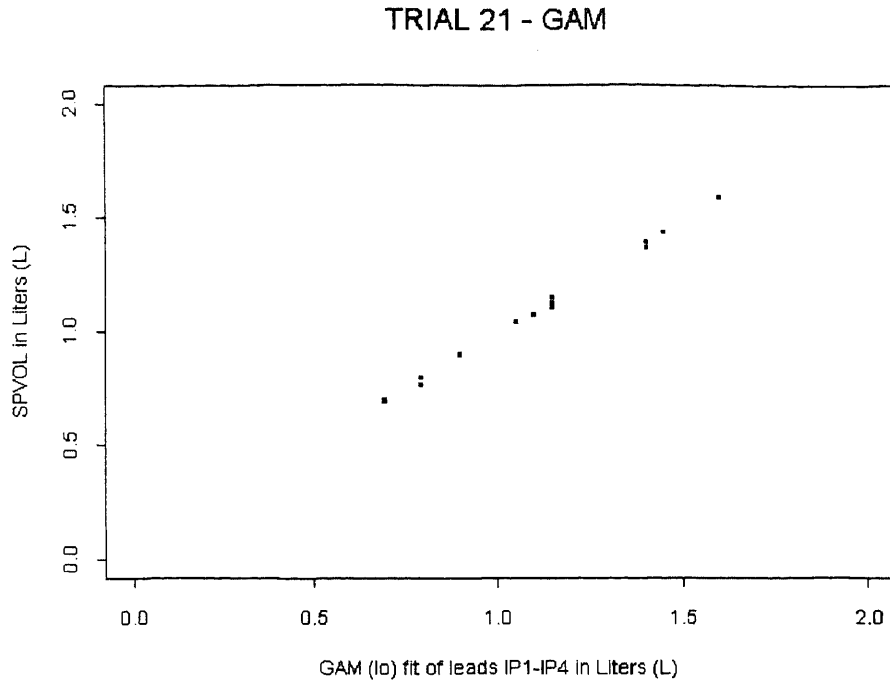
TRIAL 21 - GAM

Figure 3.5.1 GAM fitted data using the lo transform function for the combination of all leads (IPDIFF of leads I,II,III and IV) for trial 21.

TRIAL 21 - GLM
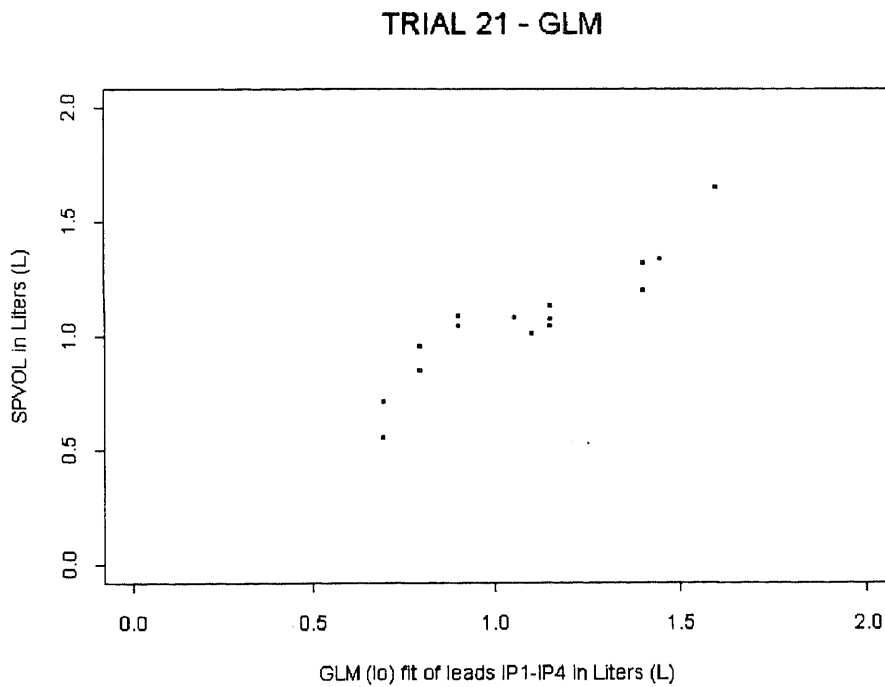
Figure 3.5.2 GLM fitted data using the lo transform function for the combination of all leads (IPDIFF of leads I,II,III and IV) for trial 21.

CHAPTER 4

RESULTS AND DISCUSSION

4.1 Results and Discussion

Data were collected from a total of 6 subjects, 3 males and 3 females, varying in age from 28 to 38. For each subject 5 sets of trial data was acquired for a total of 30 trials identified as trial 11 through trial 40. For each subject there is one trial of data for each of the clinical protocol methods identified as random, paced 8, paced 12, paced 18 and paced 8,12,18. The data file for trial 15 (subject 1, paced 8,12,18) was later found to be corrupted and unusable. Trial numbers for each subject and their associated protocol are shown in table 4-1.

Table 4-1 Clinical trial designations (trial #'s).

SUBJECT	RANDOM	PACED 8	PACED 12	PACED 18	PACED 8,12,18
1 - female, age 28	11	12	13	14	15 - N/A
2 - female, age 32	16	17	18	19	20
3 - male, age 34	21	22	23	24	25
4 - male, age 37	26	27	28	29	30
5 - male, age 33	31	32	33	34	35
6 - female, age 35	36	37	38	39	40

The data file for each trial was loaded into MATLAB with the RUNTRIAL program and processed by the signal processing programs it called. Output data was saved as trial**.mat (** = trial #) files for future processing. For each trial, the signal

processing programs generated two sets of output data, SPVOL and IPDIFF. The

SPVOL data was a single matrix of spirometer volumes in liters, for each breath identified

by a breath number. The IPDIFF data (IP1DIFF, IP2DIFF, IP3DIFF AND IP4DIFF) was

the impedance pneumograph (IP) difference data for each of the four leads. Data for each

lead was a matrix of the expiration peak to valley differences in volts for each breath

identified by breath numbers that corresponded to breath numbers in the SPVOL data.

Plots of these data for trial 21 are combined in figure 4.1, where each lead is represented

by a different symbol. As can be observed from the figure, each IP lead yields different

amplitudes for any given breath.
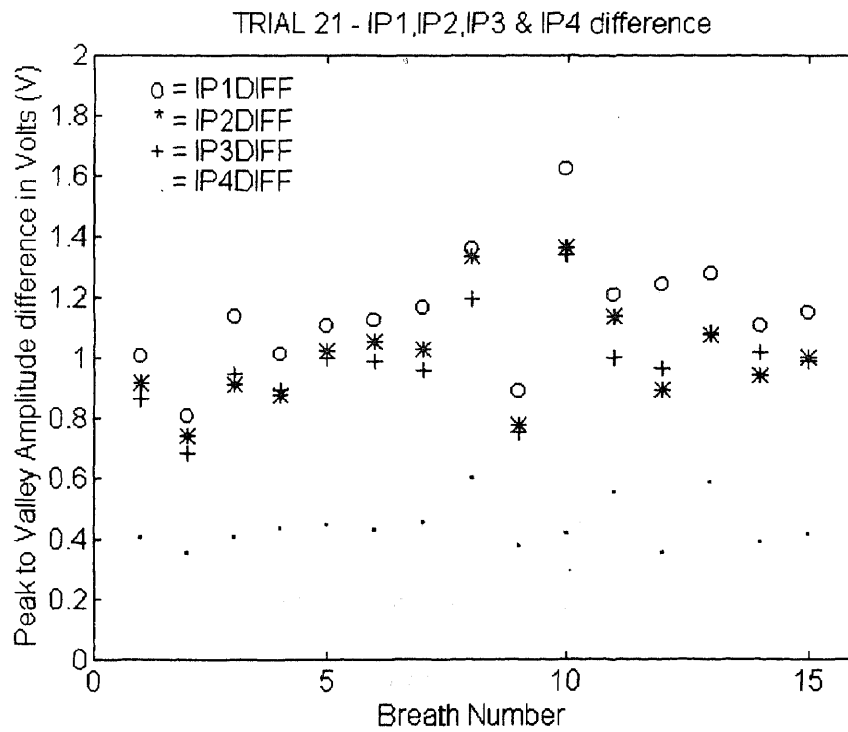
Figure 4.1 IPDIFF, peak-valley differences.

Data analysis was necessary do determine which IP lead or combination of leads would provide the best correlation to the SPVOL data. Since it was not known what combinations of the IPDIFF data or what the weights for each lead should be (i.e. what the contribution of each lead is), the data was analyzed for each lead independently and for two methods of combining the IPDIFF leads. The two combination methods were; calculating a simple mean using the IPMEAN program in MATLAB (no model, mean of IPDIFF leads) and modeling in S-Plus with GAM and GLM functions. In addition, different transform functions for the GAM and GLM were tested, including no function, s, poly and lo transforms in order to determine the optimal model. For each of the analysis methods, the SPVOL data was used as the accepted standard to which the results were compared. The IPMEAN program listing used in MATLAB and examples of functions used in S-Plus are provided in appendix 3.

As a preliminary analysis, the mean of the IPDIFF data was determined by running the IPMEAN program in MATLAB. The correlation coefficients for the individual leads IP1DIFF, IP2DIFF, IP3DIFF, IP4DIFF and IPMEAN Vs SPVOL were calculated using the MATLAB function "coorcoef" and are shown in table 4-2 as r1, r2, r3, r4 and rm respectively. It can be seen from the correlation coefficients r1-r4 and rm, that the results are not consistent, some show good correlation's (above 0.7) while most are poor (below 0.5). Although there is no supported basis for weighting the individual leads as a mean, the results do show that correlations for IPMEAN (rm) are generally better than those for the individual leads. This lends support to the rational for applying the GAM and GLM functions which combine the IPDIFF lead data and determine the best weights for each.

Table 4-2 Correlation coefficients (r) for the non-modeled IPDIFF data for each lead independently and IPMEAN.

	Correlation coefficients for the non-modeled IPDIFF data				
Trial No.	IP1DIFF r1	IP2DIFF r2	IP3DIFF r3	IP4DIFF r4	IPMEAN rm
11	0.922	0.798	0.799	0.904	0.907
12	0.577	-0.529	-0.2249	0.390	0.243
13	0.628	0.335	-.0092	0.708	0.790
14	0.833	0.497	0.473	-0.036	-0.748
15	N/A	N/A	N/A	N/A	N/A
16	0.678	0.638	0.526	0.608	0.628
17	-0.255	-0.694	-0.718	-0.697	-0.710
18	0.410	-0.090	0.031	0.053	0.042
19	0.219	0.292	0.131	0.375	0.295
20	0.745	-0.141	-0.489	0.263	-0.032
21	0.890	0.764	0.993	0.405	0.850
22	0.945	-.735	0.752	0.621	0.838
23	0.338	0.351	0.415	0.219	0.366
24	0.320	0.385	0.131	0.394	0.264
25	0.919	0.964	0.970	0.937	0.963
26	-0.377	-0.050	-0.052	0.569	-0.075
27	-0.239	-0.038	-0.014	0.218	-0.027
28	-0.090	0.026	-0.457	0.128	-0.118
29	-0.313	0.416	0.343	0.077	0.194
30	-0.047	0.708	0.789	0.774	0.584
31	0.976	0.955	0.913	0.036	-.941
32	0.932	0.855	0.817	0.217	0.935
33	0.453	0.695	0.444	-0.040	0.589
34	0.535	0.596	0.191	0.154	0.507
35	0.527	0.503	0.493	0.519	0.560
36	0.723	0.646	0.585	0.256	0.634
37	0.248	0.733	0.741	0.000	0.632
38	0.081	0.518	0.524	0.532	0.484
39	0.392	0.632	0.592	0.513	0.615
40	0.800	0.854	0.852	0.211	0.846

The SPVOL and IPDIFF data for each trial was loaded into S-Plus with the "scan" function and several versions of the models were run in order to determine which model provides the best fit. The criterion for the best fit was the model which consistently provides the lowest residual deviances. The GAM was tested first with no transform function for each IP lead individually and for lead combinations IP1+IP2, IP1+IP2+IP3, IP1+IP2+IP3+IP4 and IP1+IP4. This was then repeated for the transform functions spline (s), poly and lo. Because the there are 30 trials and there are 32 possible combinations to test for each trial, only the random trial for each subject was used to test the various iterations on the GAM function. The results of the GAM function applied to the "random" trials are provided in tables 4-3 to 4-8, from which observations can be immediately observed. The first observation is that the GAM models which included all four IP leads consistently provided the lowest residual deviations. The second observation is that the lo transform for the models which included all four IP leads (high-lighted data) provided the lowest residual deviation as compared to the other transforms in all but one case. The third observation is that the poly transform provided the same results as that of no transform function.

Table 4-3 Residual deviances for different transform functions used with GAM for several IP data combinations - Subject 1, Random.

GAM transform	IP1	IP2	IP3	IP4	IP1,IP2	IP1,IP2, IP3	IP1,IP2, IP3,IP4	IP1,IP4
No funct.	1.487	3.599	3.595	1.805	1.462	1.461	1.461	1.314
Spline (s)	0.936	2.774	1.774	0.683	0.188	0.095	0.093	0.215
Poly	1.487	3.599	3.595	1.805	1.462	1.461	1.314	1.392
lo	1.253	3.210	2.396	1.206	0.715	0.443	0.363	1.030

Table 4-4 Residual deviances for different transform functions used with GAM for several IP data combinations - Subject 2, Random.

GAM transform	IP1	IP2	IP3	IP4	IP1,IP2	IP1,IP2, IP3	IP1,IP2, 1P3,IP4	IP1,IP4
No funct.	4.37	4.79	5.85	5.10	4.31	3.89	3.85	4.36
Spline (s)	4.05	3.90	5.22	4.30	3.21	2.53	1.93	3.41
Poly	4.37	4.79	5.85	5.10	4.31	3.89	3.85	4.36
lo	4.05	4.28	5.03	4.48	3.52	2.07	1.49	3.55

Table 4-5 Residual deviances for different transform functions used with GAM for several IP data combinations - Subject 3, Random.

GAM transform	IP1	IP2	IP3	IP4	IP1,IP2	IP1,IP2, IP3	IP1,IP2, 1P3,IP4	IP1,IP4
No funct.	0.236	0.473	0.249	0.952	0.229	0.199	0.191	0.236
Spline (s)	0.169	0.423	0.182	0.836	0.133	0.071	0.025	0.111
Poly	0.236	0.473	0.249	0.952	0.229	0.199	0.191	0.236
lo	0.082	0.437	0.136	0.869	0.048	0.008	0.003	0.064

Table 4-6 Residual deviances for different transform functions used with GAM for several IP data combinations - Subject 4, Random.

GAM transform	IP1	IP2	IP3	IP4	IP1,IP2	IP1,IP2, IP3	IP1,IP2, 1P3,IP4	IP1,IP4
No funct.	0.115	0.133	0.133	0.090	0.112	0.108	0.074	0.082
Spline (s)	0.077	0.095	0.083	0.082	0.068	0.057	0.044	0.058
Poly	0.115	0.133	0.133	0.090	0.112	0.108	0.074	0.082
lo	0.056	0.078	0.064	0.080	0.038	0.029	0.018	0.039

Table 4-7 Residual deviances for different transform functions used with GAM for several IP data combinations - Subject 5, Random.

GAM transform	IP1	IP2	IP3	IP4	IP1,IP2	IP1,IP2, IP3	IP1,IP2, 1P3,IP4	IP1,IP4
No funct.	0.136	0.253	0.480	2.880	0.124	0.058	0.024	0.051
Spline (s)	0.066	0.183	0.201	0.661	0.021	0.014	0.005	0.013
Poly	0.136	0.253	0.480	2.880	0.124	0.058	0.024	0.051
lo	0.065	0.187	0.164	1.670	0.015	0.011	0.000	0.0005

Table 4-8 Residual deviances for different transform functions used with GAM for several IP data combinations - Subject 6, Random.

GAM transform	IP1	IP2	IP3	IP4	IP1,IP2	IP1,IP2, IP3	IP1,IP2, 1P3,IP4	IP1,IP4
No funct.	0.554	0.677	0.766	1.080	0.554	0.514	0.514	0.552
Spline (s)	0.481	0.538	0.605	0.972	0.358	0.311	0.291	0.412
Poly	0.554	0.677	0.766	1.080	0.554	0.514	0.514	0.552
lo	0.429	0.583	0.549	0.946	0.372	0.276	0.199	0.316

Models using the GLM function were tested in a similar fashion as that of the GAM. The GLM was tested first with no transform function for each IP lead individually and for lead combinations IP1+IP2, IP1+IP2+IP3, IP1+IP2+IP3+IP4 and IP1+IP4. This was then repeated for transform functions spline (s), poly and lo. From the results shown in tables 4-9 and 4-10, it can observed that the residual deviances for the GLM function were the same as the no transform GAM data in all cases, regardless of transform.

Table 4-9 Residual deviances for different transform functions used with GLM for several IP data combinations - Subject 1, Random.

GLM transform	IP1	IP2	IP3	IP4	IP1,IP2	IP1,IP2, IP3	IP1,IP2, 1P3,IP4	IP1,IP4
No funct.	1.487	3.599	3.595	1.805	1.462	1.461	1.461	1.314
Spline (s)	1.487	3.599	3.595	1.805	1.462	1.461	1.461	1.314
Poly	1.487	3.599	3.595	1.805	1.462	1.461	1.461	1.314
lo	1.487	3.599	3.595	1.805	1.462	1.461	1.461	1.314

Table 4-10 Residual deviances for different transform functions used with GLM for several IP data combinations - Subject 3, Random.

GLM transform	IP1	IP2	IP3	IP4	IP1,IP2	IP1,IP2, IP3	IP1,IP2, 1P3,IP4	IP1,IP4
No funct.	0.236	0.473	0.249	0.952	0.229	0.199	0.191	0.236
Spline (s)	0.236	0.473	0.249	0.952	0.229	0.199	0.191	0.236
Poly	0.236	0.473	0.249	0.952	0.229	0.199	0.191	0.236
lo	0.236	0.473	0.249	0.952	0.229	0.199	0.191	0.236

Based on these findings, it was determined that the GAM function used with the lo transform (GAM-lo), for the combination of all leads (IP1-IP4), is the model of choice to consistently provide the lowest residual deviations and therefore the best fit of the IP data to the SPVOL data. This model was applied to the remainder of the trial data along with the no transform model for the individual IP leads and the lead combinations for comparison purposes. Results provided in table 4-11 show that the GAM-lo results yielded residual deviances in the range of three to over 100 times smaller than the non-modeled results.

In order to simplify comparison of the GAM-lo (all leads) model results in S-Plus to the results from the simple IPMEAN calculations in MATLAB, the "fitted" coefficients from S-Plus were extracted, saved in ASCII format using the "write" function and loaded into MATLAB. Once in MATLAB the correlation coefficients for the S-Plus (GAM-lo) modeled data Vs SPVOL were calculated. As can be seen from table 4-12, the correlation coefficients for the modeled data (rs) were excellent. Almost all the data was greater that 0.90 and many were greater than 0.98. The results of the correlation coefficients for IPMEAN (rm) Vs. SPVOL were retabulated in table 4-13 for comparison between the two methods. From the results it is apparent that modeling of the IP data (all leads combined) using the GAM-lo function provides very good correlations to the spirometer volume data (SPVOL).

The results thus far only demonstrates the fact that data from the four IP leads can be combined using non-linear modeling such that the fitted result correlates very well with the spirometer data. Additional research is necessary determined if the weighting

coefficients for each lead are consistent for different trials on a particular subject, or if additional modeling is required. This information is crucial to determining if tidal volumes can be measured consistently and accurately in the absence of the spirometer.

Table 4-11 Residual deviances for modeling of each trial using GAM, first with no transform function and secondly for GAM-lo (combination of all four leads only).

Trial No.	GAM - (no function)					GAM- (lo)
	IP1	IP2	IP3	IP4	IP1,IP2, IP3,IP4	IP1,IP2, IP3,IP4
11	1.487	3.599	1.805	1.462	1.314	0.363
12	0.195	0.210	0.274	0.247	0.136	0.0008
13	0.122	0.180	0.201	0.101	0.019	0.0005
14	0.088	0.217	0.223	0.288	0.054	0.013
15	N/A	N/A	N/A	N/A	N/A	N/A
16	4.37	4.79	5.85	5.10	3.85	1.49
17	0.487	0.269	0.252	0.267	0.187	0.0008
18	0.669	0.798	0.804	0.802	0.578	0.113
19	0.453	0.436	0.468	0.409	0.396	0.172
20	0.509	1.12	0.870	1.06	0.442	0.102
21	0.236	0.473	0.249	0.952	0.191	0.003
22	0.169	0.737	0.696	0.986	0.160	0.009
23	3.54	3.50	3.30	3.80	3.128	1.463
24	1.919	1.821	2.10	1.806	0.80	0.198
25	0.870	0.390	0.327	0.682	0.307	0.160
26	0.115	0.133	0.133	0.090	0.074	0.018
27	0.024	0.025	0.025	0.024	0.022	0.000
28	0.080	0.081	0.064	0.079	0.057	0.011
29	0.047	0.043	0.046	0.052	0.039	0.007
30	0.241	0.120	0.091	0.097	0.073	0.044
31	0.136	0.253	0.480	2.88	0.024	0.000
32	0.079	0.162	0.201	0.578	0.059	0.0005
33	1.22	0.796	1.23	1.54	0.614	0.102
34	1.26	1.14	1.71	1.73	1.03	0.339
35	0.679	0.702	0.722	0.687	0.624	0.166
36	0.554	0.677	0.766	1.08	0.514	0.199
37	0.122	0.060	0.058	0.130	0.050	0.001
38	0.075	0.055	0.055	0.054	0.051	0.005
39	0.095	0.068	0.073	0.083	0.066	0.024
40	0.120	0.090	0.091	0.320	0.087	0.020

Table 4-12 Correlation coefficients (rs) of GAM-lo for IP1 + IP2 + IP3 + IP4 Vs SPVOL.

SUBJECT	RANDOM	PACED 8	PACED 12	PACED 18	PACED 8,12,18
1	0.992	0.998	0.998	0.976	N/A
2	0.908	0.999	0.931	0.810	0.955
3	0.998	0.997	0.810	0.952	0.986
4	0.931	0.999	0.936	0.938	0.904
5	1.000	0.999	0.968	0.902	0.915
6	0.913	0.994	0.963	0.886	0.969

Table 4-13 Correlation coefficients (rm) of IPMEAN Vs SPVOL.

SUBJECT	RANDOM	PACED 8	PACED 12	PACED 18	PACED 8,12,18
1	0.907	0.243	0.790	0.748	N/A
2	0.629	-0.711	0.042	0.293	-0.033
3	0.851	0.839	0.366	0.265	0.963
4	-0.076	-0.027	-0.118	0.194	0.584
5	0.941	0.935	0.589	0.507	0.559
6	0.634	0.632	0.484	0.615	0.846

CHAPTER 5

CONCLUSIONS AND SUGGESTIONS

5.1 Conclusions

The multi-lead TTI pneumograph device that was developed in this study worked very well from a hardware and software standpoint, providing data from four simultaneously acquired respiration leads, a lead II ECG and spirometer readings. Results of the analyzed data shows that information from the respiration lead data can be combined in a manner such that the result corresponds well with the spirometer data when processed in conjunction with it. Further, it was determined that the best correlation results were obtained when the combination of all four of the respiration leads together were modeled using the GAM-lo function.

The study met its main objective, to design, build and test a device that can be used to measure both electrocardiogram (ECG) and respiratory tidal volume, although additional work is needed to make the device useful for actual HRV study applications. For use in HRV studies the device must determine tidal volume in the absence of a spirometer. The results of this study suggest that there is sufficient information within the respiration lead data for this to be possible. Additional data processing is needed in order to use the modeling results obtained in this study, to obtain for each subject, a best fit model that is not spirometer dependent. In this way, for each subject, a model can be created during a calibration phase using a spirometer and then be applied to impedance

data on successive trials with the spirometer removed. The quality of the fit will determine the accuracy of the tidal volume determinations.

5.2 Suggestions

As this study focused on the development of the multi-lead TTI pneumographic device, many questions have been answered, but additional data analysis is necessary make the overall method useful for HRV studies. Suggestions for future research includes the following:

- Continue the development of the data analysis modeling so that the tidal volume may be determined in the absence of a spirometer. Ideally, the spirometer should only be used for calibration purposes at the beginning of trials for each subject.

- It was suspected that errors introduced for low tidal volumes that may have affected some of the results. This may be due to signal to noise considerations since low volumes produce much lower impedance signals. This spirometer is a known source of error since it only has a resolution of only 50 mL. This can lead to large percentage errors for low tidal volumes. It is strongly recommended that another type of spirometer be used, one which has a much finer resolution for measuring small volume changes and possibly both inspiration and expiration volume readings.

- Testing with additional subjects is recommended to better validate the results obtained in this study.

- As part of their clinical protocol, researchers may wish to include the subjects in different postures such as standing or lying down, as well as tests involving motion such as cycling or walking.

- If it is determined that noise from motion artifacts overly corrupts the data, it may be desirable to modify the hardware to convert the multi-lead TTI pneumograph circuitry from a bipolar to a tetra polar configuration.

- Further investigations should attempt to minimize the number of leads required in order to simplify the clinical protocol and increase patient comfort yet maintain good data.

- Investigate the many variables associated with different electrode types as well as electrode placement sites and preparation for possible improvements.

APPENDIX 1

Engineering Drawings
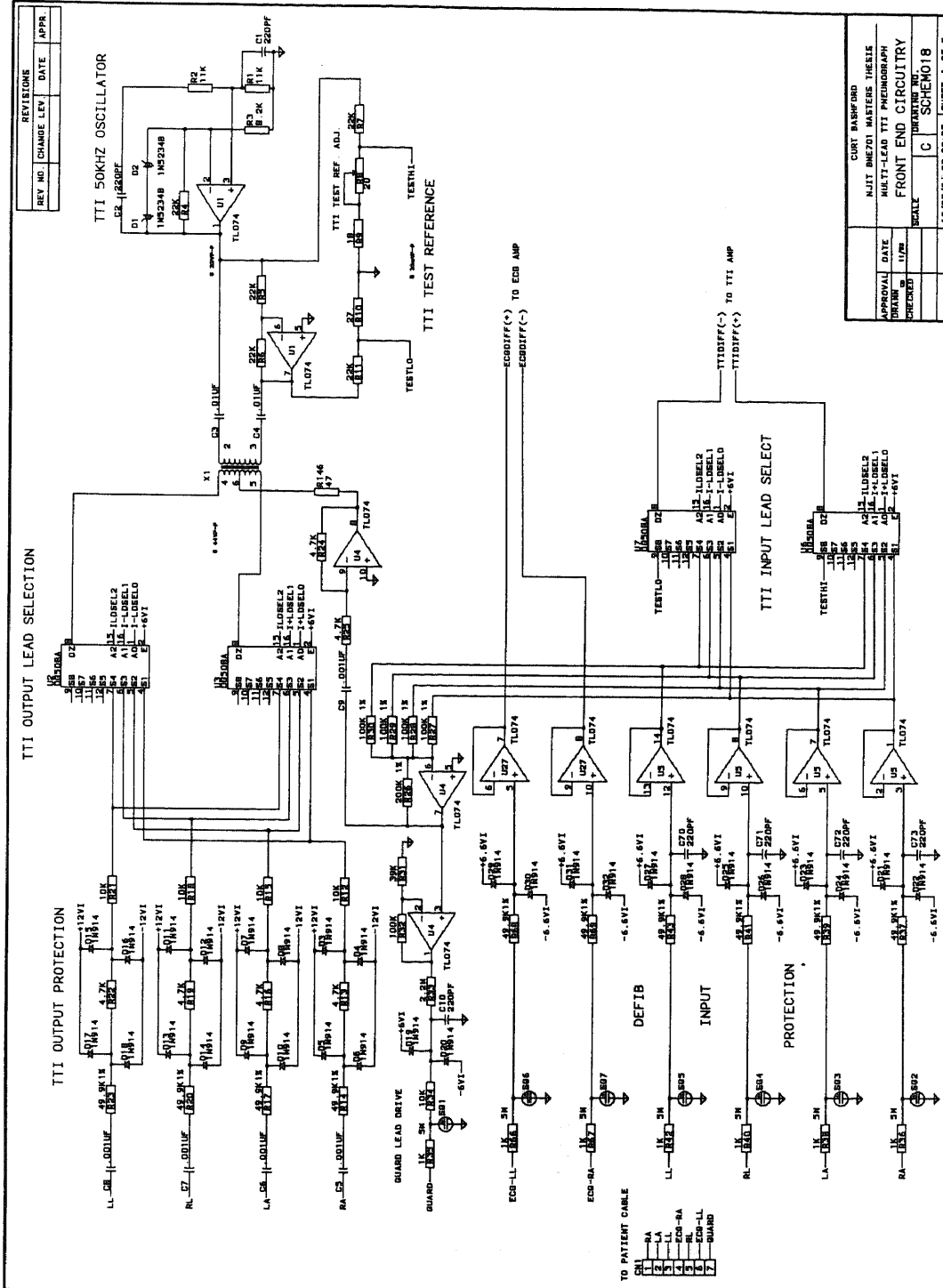
Front-End Schematic - 1 of 5

Front-End Schematic - 2 of 5

Front-End Schematic - 3 of 5

Front-End Schematic - 4 of 5
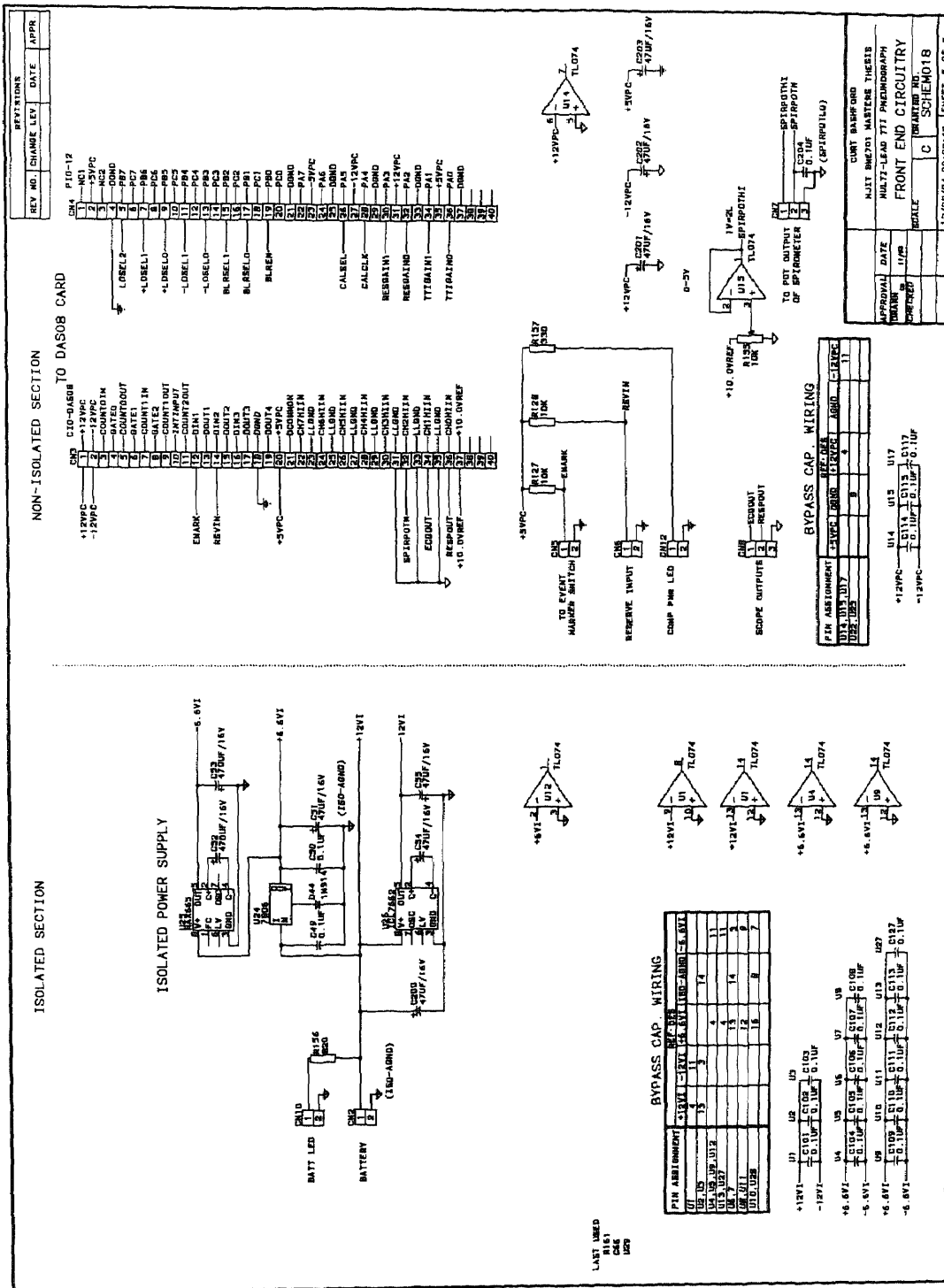
Front-End Schematic - 5 of 5
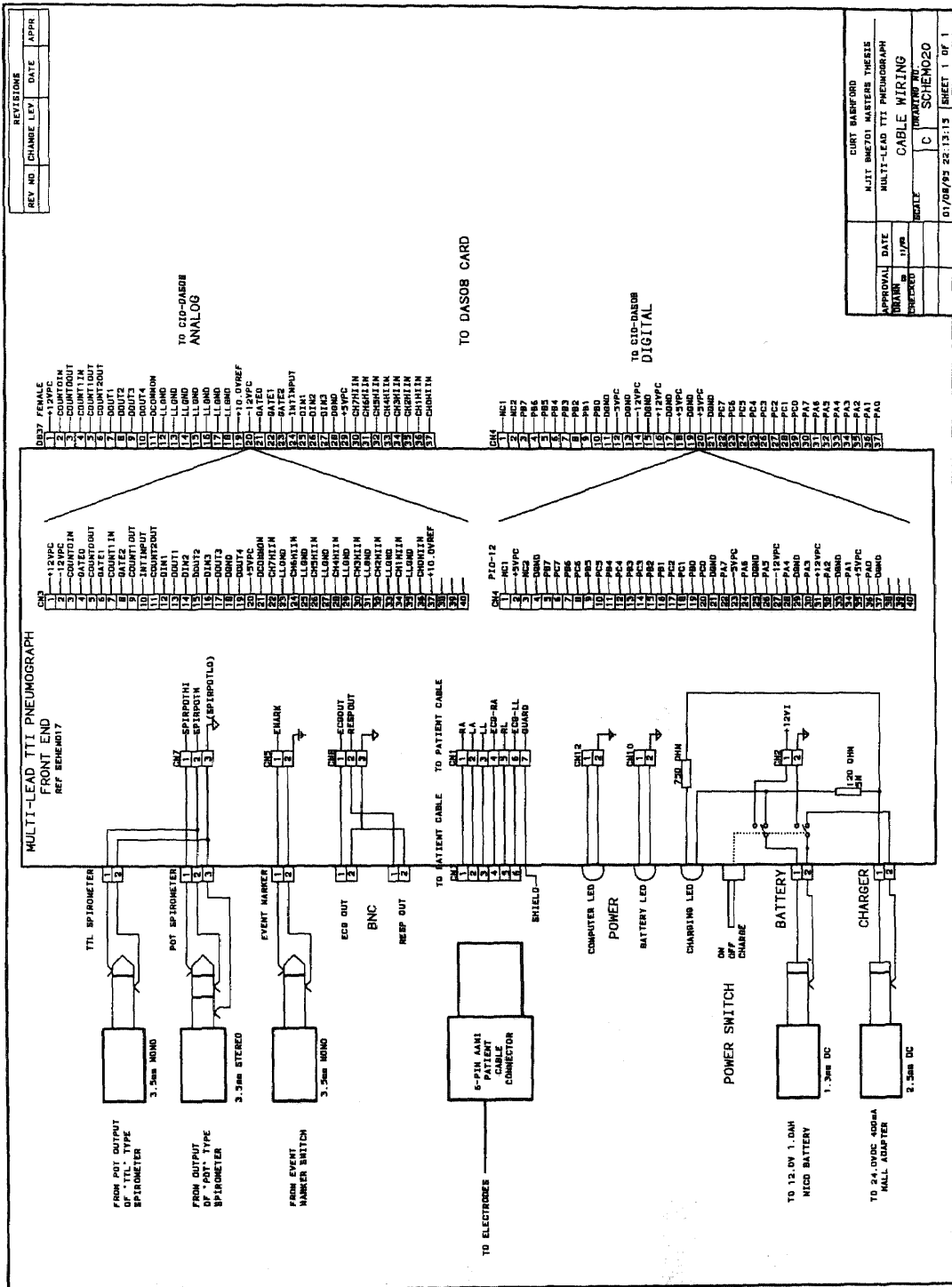
Front-End Cable wiring - 1 of 1
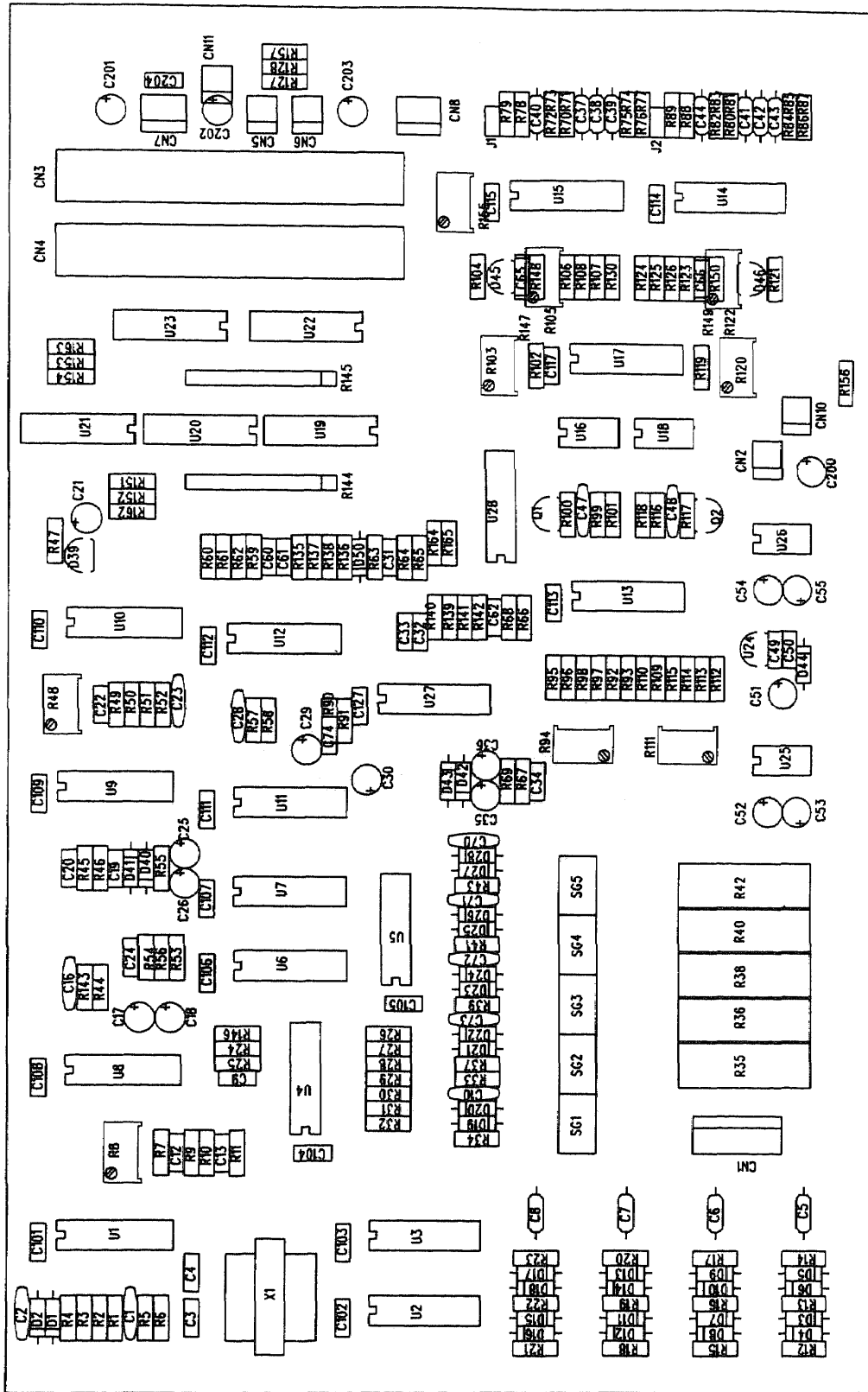
Front-End Assembly Drawing - Main bd.

R200

C210
C211
R201
C212
C213

C131
C217
C216
R204
R205
R206
R207
C215
U31
D101
R202
R203
C214

R210

C220
C221
R211
C222
C223

C132
C227
C226
R214
R215
R216
R217
C225
U32
D103
R212
R213
C224

R220

C230
C231
R221
C232
C233

C133
C237
C236
R224
R225
R226
R227
C235
U33
D105
R222
R223
C234

C130

U30

R230

C240
C241
R231
C242
C243

C134
C247
C246
R234
R235
R236
R237
C245
U34
D107
R232
R233
C244

CN13

Front-End Assembly Drawing - BLR bd.
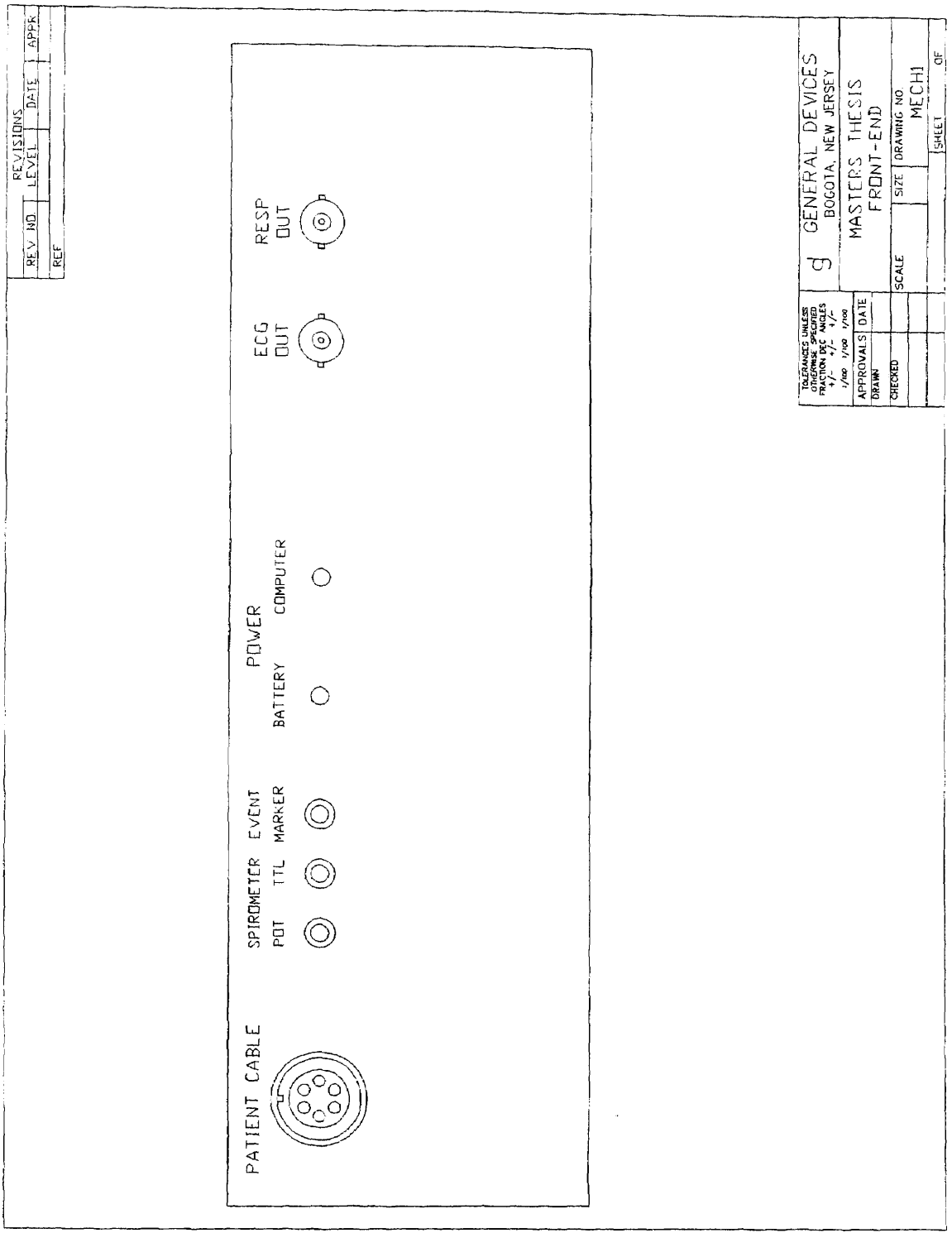
Front-End Enclosure - Front Panel
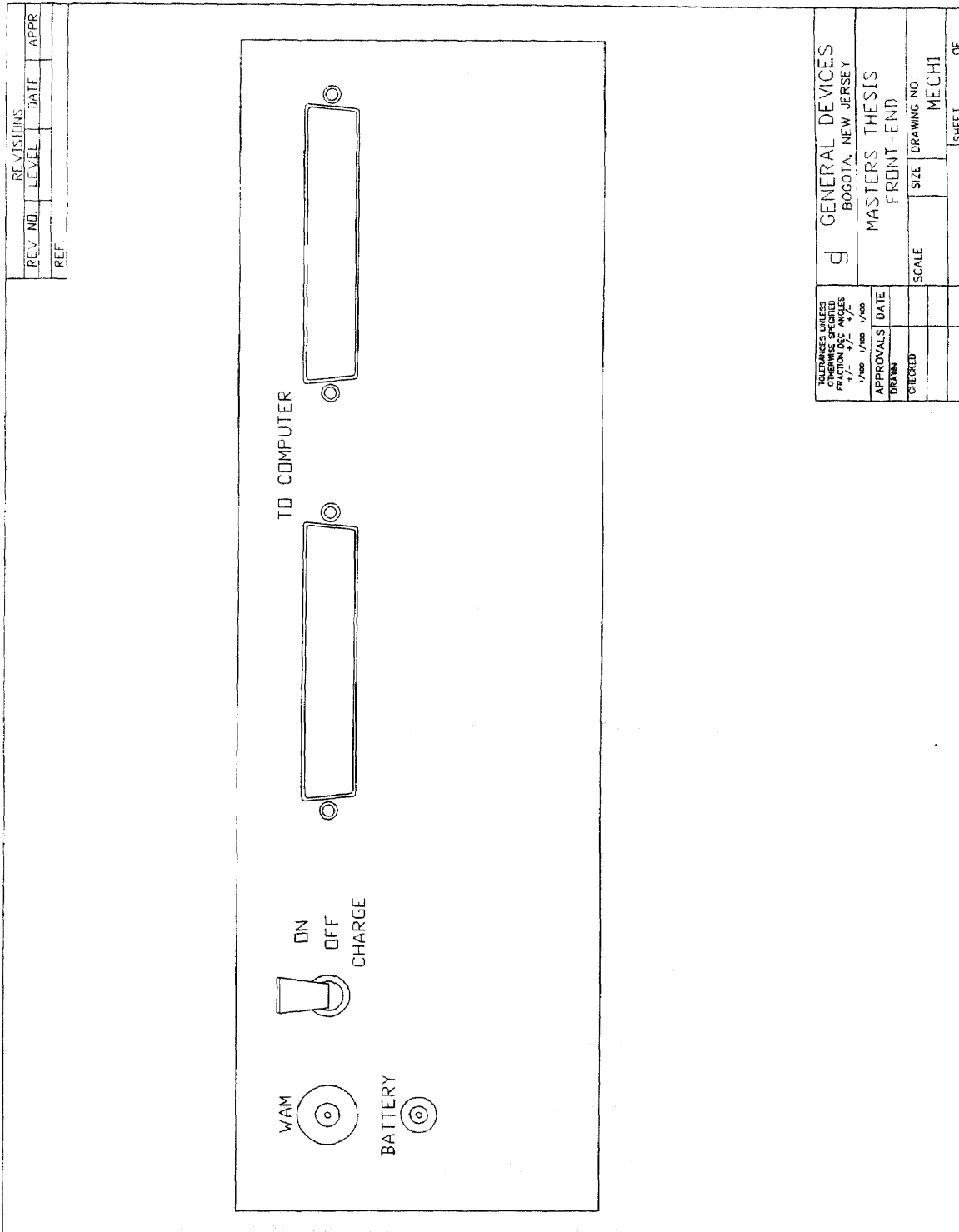
Front-End Enclosure - Rear Panel

APPENDIX 2

Front End Theory of Operation

A2.1 Overview

The front end circuitry is divided into five main sections, the respiration channel, the ECG channel, the spirometer channel, control logic and power supply. Each section is organized by functional blocks. For better understanding, refer to figure 2.3.1 in section 2.3 and the schematics located in appendix 1.

A2.2 Theory of Operation - Respiration Channel

A2.2.1 TTI 50 Khz Oscillator

The TTI oscillator composed of U1-A and its associated components is a form of a Wein-bridge oscillator. The frequency of oscillation is set by the RC pairs R1-C1 and R2-C2. The output of U1-A is a quasi-sinewave at 50 Khz with an amplitude of 22VP-P. This signal is applied to the x1 inverter U1-B and is also AC coupled to one side of the primary of transformer XFMR1. The output of U1-B is AC coupled to the other side of the primary of XFMR1 to form a bridge type differential drive. The transformer XFMR1 provides a relatively constant load for the oscillator which is required to prevent it from stopping from running due to load changes. The secondary of XFMR1 is center tapped with the tap being driven with a guard signal common for noise reduction. The two outputs of the secondary provide the 50 Khz TTI oscillator signal at 44VP-P to the TTI output lead select circuitry. The outputs of U1-A&B are also applied to the TTI Test

Reference circuit which is formed by the differential divider of R7 through R11. This test reference signal is trimmed by pot. R8 and can be used for calibration and test purposes.

A2.2.2 TTI Output Lead Selection and Defibrillation Protection

The secondary of transformer XFMR1 is applied to the commons of analog switches U2 and U3. These DG508A switches are 1:8 multiplexers with make before break operation that can operate on supplies up to +/-18V. The four low order outputs of both U2 and U3 are wired common so that the differential signal can be selectively applied to any combination of the four respiration electrodes. Independent selection of the (+) and (-) outputs is provided for by the separate control lines I+LDSEL* and I-LDSEL*. The four outputs are protected from defibrillation potentials by the diode clamping network of D3 through D18. The series output resistors R12 through R23 provide current limiting for patient safety and clamping as well as a high source impedance for the TTI oscillator. In this way, the TTI oscillator appears as a constant current source since the voltage is high and the source impedance is high as compared to the low load impedance the body presents. The outputs are AC coupled to the patient cable electrodes by capacitors C5,C6,C7 and C8.

A2.2.3 TTI Input Lead Selection and Defibrillation Protection

Inputs from the respiration electrodes are first protected against defibrillation potentials by spark-gaps SG1-SG5 and current limiting resistors R36,R38,R40 and R42 which limit the

signal to 90V. The diode clamping circuits at the inputs of input buffers U5-A, U5-B, U5-C and U5-D perform further protection by clamping to the +/- supply rails.

A2.2.4 Guard Lead Drive

The outputs of buffers U5-A,B,C and D are summed together at the X2 summing amplifier U4-B. The output of U4-B is AC coupled to the X1 inverter of U4-C whose output is applied to the center tap of transformer XFMR1. The output of U4-B is also applied to the X3.5 non-inverting amplifier of U4-A. The output of U4-A is current limited by R33 and protected from defibrillation potentials by diode clamps D19 and D20 along with spark gap SG1 and R35.

A2.2.5 TTI Input Lead Select and Instrumentation Amplifier

The TTI input selection operates in the same way as the output selection. U6 and U7 are DG508A 1:8 multiplexers with their four low order inputs wired common so that the differential signal can be selected from any combination of the four respiration input buffers. Independent selection of the (+) and (-) inputs is provided for by the same control lines as the output selection (I+LDSEL* and I-LDSEL*) so that the input selection automatically matches the output selection. The TTI test reference signal is applied to input 8 of U6 and U7 for test purposes. The selected outputs of U6 and U7 are applied to the input of the TTI instrumentation amplifier U11. Amplifier U11 was chosen as an INA110 because it can handle the high frequency TTI signal and provides a relatively clean output. The gain of U11 is configured for X10 by connecting U11-3 to U11-13.

A2.2.6 X-10 and Programmable TTI Gain

The output of U11 is AC coupled to the fixed gain X-10 amplifier of U12-B whose output is applied to the programmable gain amplifier of U12-D. The TTI gain is set by analog switches U10-A and U10-B which switch in resistors in parallel to the feedback resistor of U12-D. The gain at U12-D is delectable as X-1, X-2 or X-4 and is controlled by control lines ITTIGAIN0 and ITTIGAIN1 for an overall gain of X100, X200 or X400 (non-inverted). This programmable gain allows the TTI signal amplitude to be optimally amplified to compensate for differences in electrode to skin impedance as needed for each patient or trial.

A2.2.7 ECG Reject HPF, Envelope Detector and 500 Hz LPF

The amplified signal from U12-D is applied to the 2-pole 1KHz high pass filter formed at U12-C which provides rejection of any ECG signal that may be riding on the recovered TTI signal. The output of U12-C is the Amplitude Modulated (AM) TTI signal. The respiration signal is actually the AM signal envelope is that which is desired from the TTI signal. To recover this information the output of U12-C is applied to the simple AM envelope detector composed of D50, R63 and the 2-pole 500Hz Low Pass Filter of U27-D. The cutoff frequency of this LPF was kept high because the respiration channel is multiplexed at a 25Hz rate with four sub channels (leads) and mixing of the channels would otherwise occur.

A2.2.8 Respiration Base-Line Recovery

The output signal of U27-D is the composite respiration signal. The respiration signal by it's nature is a very low frequency signal that may have base-line wander due to such factors as motion artifact. Because of the relatively high gain in the circuitry, it is necessary to have Base-Line Recovery (BLR) to limit this wander and prevent the signal from going into saturation. Simple AC coupling is not acceptable, active circuitry is required. In addition, because there are four respiration leads that are multiplexed onto the single respiration channel by switching the lead selection during acquisition, the individual respiration sub-channels each require their own BLR circuits.

The composite respiration signal from U27-D is applied to the common of U30-A which is a dual 1:4 analog switch. The input common is switched to the appropriate one of four BLR channels by the IBLRSEL* controls. Each BLR channel consists of a sample and hold, a 2-pole 25Hz low pass filter and BLR circuit. The first respiration sub-channel is inputted to the sample and hold circuit consisting of C210 and buffer U31-A. This circuit holds the signal when the input is switched to the other BLR channels in order to minimize decay of the BLR signal. The output of U31-A is filtered with the 2-pole 25Hz LPF circuit of U31-B to remove unwanted noise outside the respiration bandwidth. The output of U31-B is inputted to U31-C as a normal inverting amplifier however, the non-inverting terminal is fed by the output of the integrator U31-D which forms a feedback loop since the input to the integrator is the output of U31-C. The effect of the integrator is to pull the output of U31-C towards 0V or baseline. There are two input paths to the BLR integrator. The normal path is through R204, where the high pass time constant is

set by the RC combination of R214 and the C216, C217 combination times the non-inverting gain of U31-C and is typical near DC at approximately 0.05Hz. The second path is a fast recovery path which speeds up the time constant for large offsets, such as when the signal goes into saturation. Fast recovery is active only when the output of U31-C is large enough such that the signal divided by R205, R207 is large enough to forward bias either D100 or D101 through R206. The recovery is speeded up because the R component of the RC combination is now R216 which is considerably lower in value than R214. The operation of BLR channels 1,2 and 3 are identical utilizing U32, U33 and U34 respectively. The outputs of the four BLR channels are applied to U30-B for multiplexed selection to the common output at U30-3. The BLR output selection controls and operation are the same as for BLR input selection so that the input and output selections automatically match. The enable input of U30 is controlled by the IBLREN line. The enable is set high for a short period to disconnect the analog switches between BLR channel selections to prevent switching transients from degrading the signals.

A2.2.9 Programmable Respiration Gain

The selected output of U30-B (BLROUT) is inputted to the programmable gain amplifier of U27-A. The respiration gain is set by analog switches U28-A and U28-B which switch in resistors R145 and R146 in parallel to the feedback resistor of U27-A (R140). The gain at U27-A is selectable as X-5, X-10 or X-20 and is controlled by control lines IRESGAIN0 and IRESGAIN1. This programmable respiration gain allows the signal

amplitude to be optimally amplified for good signal to noise without causing saturation as needed for each patient or trial.

A2.2.10 Respiration Opto-Isolator Input

The selected output of U27-A (ISORESP) is inputted through divider R109-R110 to the amplifier of U13-B where a DC offset bias is injected. The output of U13-B is 0.2X ISORESP and potentiometer R111 is adjusted for a +0.51V offset at U13-7 so that the signal is scaled and biased within the opto-isolator's linear region. This signal is applied to the opto drive circuit of U13-C which drives optocoupler U18's LED with feedback from it's internal feedback photodiode. The linear optocoupler provides the required electrical isolation as it is only optically coupled to its output photodiode

A2.2.11 Respiration Opto-Isolator Output

The signal received at the output photodiode of U18 is inputted to the variable gain amplifier of U17-B. Potentiometer R120 is adjusted for a X1 gain at U17-7 with respect to U13-7. The output of U17-B is inputted to noninverting amplifier U17-C where the offset is null'ed by adjusting potentiometer R122. The output signal of U17-C is further amplified by the X2 noninvertring amplifier of U14-A which gives an overall gain of X2 for the transfer of signal ISORESP from the isolated to the non-isolated circuitry.

A2.2.12 Respiration 60Hz Notch Filter

The circuitry of U14-C&D forms a driven Twin-T notch filter. The frequency setting components were precisely measured and selected to achieve a very high Q response with the notch centered at 60Hz. This circuit provides additional 60Hz noise rejection if needed or can be bypassed by jumping J2 pin 1 to pin 2. For this study the notch filter was bypassed because the high frequency of the multiplexed signal caused ringing.

A2.2.13 Respiration Output

The respiration output signal RESPOUT is wired to the front panel RESP OUT BNC jack and to the DB37 connector for connection to the CIO-DAS08 card at A/D CH0. This signal is time-division multiplexed with the respiration signals from the four respiration leads (electrode pairs). It is bipolar with a full scale of +/-5V and a typical signal amplitude of 0.5 to 2VP-P.

A2.3 Theory of Operation - ECG Channel

A2.3.1 ECG Input Defibrillation Protection and Buffers

Inputs from the ECG electrodes (ECG-RA & ECG-LL) are first protected against defibrillation potentials by spark-gaps SG6 and SG7 and current limiting resistors R66 and R67 which limit the signal to 90V. The diode clamping circuits at the inputs of input buffers U27-B and U27-C perform further protection by clamping to the +/- supply rails.

A2.3.2 ECG Instrumentation Amplifier and 100Hz LPF

The outputs of buffers U27-B and U27-C (ECGDIFF(+/-) are applied to the input of the

ECG instrumentation amplifier U8. Amplifier U8 is a low-power high-accuracy

instrumentation amplifier that provides a minimum of 90dB of common mode rejection.

The gain of U8 is configured for X10 by connecting U8-2 to U8-6 and U8-7. The output

of U8 is filtered by the 2-pole unity gain 100Hz Low Pass Filter (LPF) which filters out

the high frequency TTI oscillator signal that is picked up at the electrodes and leaves the

ECG signal.

A2.3.3 Calibration Generator and Select Switch

Voltage reference D39 provides a -1.25V reference to pin 4 of analog switch U10-C. The

output of U10-C is divided by the divider network of R48, R49 and R50 and inputted to

the inverting input of X50 amplifier U9-C. The noninverting pin of U9-C is sourced by

the common of analog switch U28-C and is selected by control line ICALSEL such that

either the filtered ECG signal from U9-A or iso-ground is applied. Potentiometer R48 is

adjusted for 0.50V at the output of U9-C (ISOECG) with both ICALSEL and ICALCLK

set to low. When the control line for U10-C (ICALCLK) is clocked and ICALSEL is set

low (Cal.), the output of U9-C is a 0 to 0.5 V calibration signal corresponding to 1mV

Relative To the Input (RTI).

A2.3.4 ECG Base Line Recovery

The output of U9-C (ISOECG) is inputted to the BLR circuit of U9-B which forms a feedback loop since the output of the BLR circuit is fed back to the COM terminal of the instrumentation amplifier. U9-B is configured as an integrator. The effect of the integrator is to pull the output of U9-C towards 0V or baseline. There are two input paths to the BLR integrator. The normal path is through R55, where the high pass time constant is set by the RC combination of R55 and the C26, C26 combination is approximately 0.5Hz. The second path is a fast recovery path which speeds up the time constant for large offsets, such as when the signal goes into saturation. Fast recovery is active only when the output of U9-C is large enough such that the signal divided by R53, R54 is large enough to forward bias either D40 or D41 through R56. The recovery is speeded up because the R component of the RC combination is now R56 which is considerably lower in value than R55.

A2.3.5 ECG Opto-Isolator Input

The output of U9-C (ISOECG) is inputted through divider R92-R93 to the amplifier of U13-A where a DC offset bias is injected. The output of U13-A is 0.2X ISOECG and potentiometer R94 is adjusted for a +0.51V offset at U13-1 so that the signal is scaled and biased within the opto-isolator's linear region. This signal is applied to the opto drive circuit of U13-D which drives optocoupler U16's LED with feedback from it's internal feedback photodiode. The linear optocoupler provides the required electrical isolation as it is only optically coupled to its output photodiode

A2.3.6 ECG Opto-Isolator Output

The signal received at the output photodiode of U16 is inputted to the variable gain amplifier of U17-A. Potentiometer R103 is adjusted for a X1 gain at U17-1 with respect to U13-1. The output of U17- A is inputted to X5 noninverting amplifier U17-D where the offset is nulled by adjusting potentiometer R105. The output signal of U17-D is further amplified by the X2 noninvertring amplifier of U15-B which gives an overall gain of X2 for the transfer of signal ISOECG from the isolated to the non-isolated circuitry.

A2.3.7 ECG 60Hz Notch Filter

The circuitry of U15-C&D forms a driven Twin-T notch filter. The frequency setting components were precisely measured and selected to achieve a very high Q response with the notch centered at 60Hz. This circuit provides additional 60Hz noise rejection if needed or can be bypassed by jumping J2 pin 1 to pin 2. For this study the notch filter was used.

A2.3.8 ECG Output

The ECG output signal ECGOUT is wired to the front panel ECG OUT BNC jack and to the DB37 connector for connection to the CIO-DAS08 card at A/D CH1. The ECG signal has an overall gain of 1000 RTI (1mV=1V) and is bipolar with a full scale of +/- 5V.

A2.4 Theory of Operation - Spirometer Channel

Because there is no electrical or conductive connections between the spirometer and patient, there are no isolation requirements and the spirometer's output is able to connect directly to the non-isolated portion of the front-end circuitry. There are two input jacks provided to accommodate two types of spirometer outputs. The 3.5mm stereo jack labeled SPIROMETER POT is for spirometers with isolated potentiometer outputs. The voltage at the input to buffer U15-A is set to +5.0V by pot R155 which forms a voltage divider on the +10.0VREF line. The output of buffer U15-A supplies the high side of the spirometer's potentiometer (SPIROPOTHI) and the low side is tied to analog ground (SPIROPOTLO). In this configuration the wiper of the spirometer's potentiometer provides a voltage between 0 and +5V corresponding to it's mechanical position which relates to respiration. This signal (SPIROPOTW) is inputted directly to A/D channel 2. Capacitor C204 provides noise suppression.

The 3.5mm mono jack labeled SPIROMETER TTL is for spirometers with TTL transition outputs. Because this type of input does not require any drive circuitry, the TTL signal (0 to +5V) is wired directly to the SPIROPOTW line and is inputted to A/D channel 2 the same as for the potentiometer type spirometer. This is allowed since only one type spirometer is used at a time.

A2.5 Theory of Operation - Control Logic

All of the front-end digital control logic, both Input and Output (I/O) is wired to the CIO-DAS08 card through the PIO DB37 cables. The I/O on the CIO-DAS08 card is provided

by an 8255 which is a programmable peripheral that has 24 bits of I/O on three ports and by four dedicated outputs and three dedicated inputs. All of the logic levels are standard TTL (0 to 5V). Fourteen bits of the programmable I/O is used as outputs for control of the front-end circuitry. One dedicated digital input (DIN1) is used and is wired directly to the event marker jack. No control logic is utilized on the non-isolated portion of the front-end circuitry and therefore must be transferred to the isolated portion. To accomplish this, the controls are inputted ULN2003 open collector drivers U22 and U23. The outputs of U22 and U23 are wired the cathodes of optocouplers U19, U20, U21 and U29 and resistor arrays R145 and R152 are wired to the anodes. When one of the outputs used from the CIO-DAS08 is TTL high, the output of the associated ULN2003 gate goes low which turns on the led of the associated optocoupler. This turns on its paired phototransistor which pulls the isolated control line low. By this gating sequence there is a net inversion of logic levels from the output of the CIO-DAS08 to the isolated control. Logic high on the isolated side is pulled up by the +6.6VI supply through resistor arrays R144 and R151. Isolated controls are labeled the same as their associated non-isolated controls with the addition of an "I" prefix to designate them as isolated.

A2.6 Theory of Operation - Power Supply

There are two power supply sections for the front-end circuitry, one for the isolated section and one for the non-isolated section. The power source for the isolated section is a single LP5 12.0V 1.0AHr NICd battery pack. The battery is external to the front-end enclosure and is connected at the 1.3mm DC jack BATTERY connector. The battery

connections are switched by the DPDT power switch where OFF disconnects the battery, ON connects the battery to the front-end circuitry and CHARGE connects the battery to the CHARGER jack through a 200 ohm current limiting resistor. To charge the battery, a 24VDC Wall Adapter Module (WAM) is connected to the 2.1mm CHARGER jack and the power switch is set to CHARGE. The current limiting resistor sets the charge rate to approximately Capacity/16 or 60mA which is a trickle charge rate and can be applied for extended periods of time. When the battery is charging, the CHARGE LED is lit.

When the power switch is in the ON position, the battery power is applied to the +12VI circuit and is indicated by the BATTERY LED. In addition to supplying some circuits directly, the +12VI supply powers linear regulator U24 and inverter U26. Regulator U24 is a positive 6V regulator with its ground reference connected through diode D44 which raises the output of U24 to 6.6V. The output of U24 is the source for the +6.6VI supply. U26 is charge-pump type voltage inverter which generates the -12VI supply by inverting the +12VI supply. The -6.6VI supply is generated similarly from the +6.6VI supply by U25 which is a high output (100mA) charge-pump inverter. These four voltage supplies power the entire isolated section of the front-end.

The power supply for the non-isolated section of the front-end circuitry is the computers switching power supply. The +12VPC, -12VPC, +5VPC, -5VPC and +10.0VREF voltages are passed through the CIO-DAS08 card and DB37 cables to the front-end. No additional regulation is required, the only circuitry is filter capacitors C201, C202 and C203. Computer power is indicated by the COMPUTER LED. The power distribution and pin-outs for the integrated circuits are shown in the two tables on page four of the front end schematic.

APPENDIX 3

Software Listings

ACQUIRE.CPP PROGRAM

```
/* ACQ2_0.CPP 10/26/94 - SPIRO @50Hz, RESP1-4 @ 25Hz, ECG AT 100Hz */

#include <graphics.h>
#include <stdlib.h>
#include <stdio.h>
#include <conio.h>
#include <dos.h>
#include <cb.h>

#define MAXSAMPLE  2250

FILE *out;
int i = 0;
int j;
int k=0;
int Datapoint = 0;
int BoardNum = 0;
int PortNum, Direction, DataValue;
char ch;

unsigned
Resp1[MAXSAMPLE],Resp2[MAXSAMPLE],Resp3[MAXSAMPLE],Resp4[MAXSA
MPLE];
unsigned ECG[8*MAXSAMPLE], Spiro[2*MAXSAMPLE];
unsigned *Resp1ptr,*Resp2ptr,*Resp3ptr,*Resp4ptr;
unsigned *ECGptr,*Spiroptr;

#define ADCBASE 0x300

void Sdelay(int interval) /* short delay, depends upon CPU speed */   ·
{ for(k=0; k<interval; k++);
}

void ADCIn(int BoardNum,int Channel,int Gain,unsigned *OUTptr) /* ADC format */
{ int k;
  outportb(ADCBASE+2,(char) Channel); /* set mux ch */
  Sdelay(1);   /* delay to allow signal to stablize from mux to ADC */
  outportb(ADCBASE+1,0); /* initiate 12bit conversion */
  k=0; while(((inportb(ADCBASE+2)&0x80)==0x80)&&(k<10000)) k++; /* test for
EOC = 0 */
  if(k<10000)
  { *OUTptr = (unsigned)(inportb(ADCBASE+1) * 256 + inportb(ADCBASE)) >> 4;
  }
```

```c
      else
      {  printf("\n          ** ERROR ** ADC Conversion fail....");
         *OUTptr = 0xffff;
         BoardNum = Gain; /* dummy code */
         Gain = BoardNum; /* dummy code */
         getch();
      }
}


void plot(void)
{  int gdriver = DETECT, gmode, errorcode;
   int xmax, ymax,xpos,ypos;
   int j;
   /* initialize graphics and local variables */
   initgraph(&gdriver, &gmode, "");
   /* read result of initialization */
   errorcode = graphresult();
   /* an error occurred */
   if (errorcode != grOk)
   {  printf("Graphics error: %s\n", grapherrormsg(errorcode));
      printf("Press any key to halt:");
      getch();
      exit(1);
   }
   setcolor(getmaxcolor());
   xmax = getmaxx();
/*   ymax = getmaxy(); */
   /* draw ECG waveform */
   outtext("ECG");
   moveto(0, 120-(long)(ECG[0])*120/4096);
   xpos=1; j=0; ypos=0;
   for(i=1; i<MAXSAMPLE*8; i++)
   { lineto(xpos,120-(long)(ECG[i])*120/4096+ypos);
     if(++xpos>=xmax)
     { j++; xpos=0; ypos=120*j; if(ypos==360) ypos--;
         moveto(0, 120-(long)(ECG[i+1])*120/4096+ypos); i++;
         if(j>3)
         { j=0;
           getch();
           clearviewport();
           moveto(0, 120-(long)(ECG[i+1])*120/4096); ypos=0;
         }
     }
   }
   getch();
```

```
/* draw Spiro waveform */
  clearviewport();
  outtext("Spiro");
  moveto(0, 120-(long)(Spiro[0])*120/4096);
  xpos=1; j=0; ypos=0;
  for(i=1; i<MAXSAMPLE*2; i++)
  { lineto(xpos,120-(long)(Spiro[i])*120/4096+ypos);
    if(++xpos>=xmax)
    { j++; xpos=0; ypos=120*j; if(ypos==360) ypos--;
        moveto(0, 120-(long)(Spiro[i+1])*120/4096+ypos); i++;
        if(j>3)
        { j=0;
          getch();
          clearviewport();
          moveto(0, 120-(long)(Spiro[i+1])*120/4096); ypos=0;
        }
    }
  }
  getch();
/* draw Resp1 waveform */
  clearviewport();
  outtext("Resp1");
  moveto(0, 120-(long)(Resp1[0])*120/4096);
  xpos=1; j=0; ypos=0;
  for(i=1; i<MAXSAMPLE; i++)
  { lineto(xpos,120-(long)(Resp1[i])*120/4096+ypos);
    if(++xpos>=xmax)
    { j++; xpos=0; ypos=120*j; if(ypos==360) ypos--;
        moveto(0, 120-(long)(Resp1[i+1])*120/4096+ypos); i++;
        if(j>3)
        { j=0;
          getch();
          clearviewport();
          moveto(0, 120-(long)(Resp1[i+1])*120/4096); ypos=0;
        }
    }
  }
  getch();
/* draw Resp2 waveform */
  clearviewport();
  outtext("Resp2");
  moveto(0, 120-(long)(Resp2[0])*120/4096);
  xpos=1; j=0; ypos=0;
  for(i=1; i<MAXSAMPLE; i++)
  { lineto(xpos,120-(long)(Resp2[i])*120/4096+ypos);
```

```c
  if(++xpos>=xmax)
  { j++; xpos=0; ypos=120*j; if(ypos==360) ypos--;
      moveto(0, 120-(long)(Resp2[i+1])*120/4096+ypos); i++;
      if(j>3)
      { j=0;
        getch();
        clearviewport();
        moveto(0, 120-(long)(Resp2[i+1])*120/4096); ypos=0;
      }
  }
  }
  getch();
/* draw Resp3 waveform */
  clearviewport();
  outtext("Resp3");
  moveto(0, 120-(long)(Resp3[0])*120/4096);
  xpos=1; j=0; ypos=0;
  for(i=1; i<MAXSAMPLE; i++)
  { lineto(xpos,120-(long)(Resp3[i])*120/4096+ypos);
    if(++xpos>=xmax)
    { j++; xpos=0; ypos=120*j; if(ypos==360) ypos--;
        moveto(0, 120-(long)(Resp3[i+1])*120/4096+ypos); i++;
        if(j>3)
        { j=0;
          getch();
          clearviewport();
          moveto(0, 120-(long)(Resp3[i+1])*120/4096); ypos=0;
        }
    }
  }
  }
  getch();
/* draw Resp4 waveform */
  clearviewport();
  outtext("Resp4");
  moveto(0, 120-(long)(Resp4[0])*120/4096);
  xpos=1; j=0; ypos=0;
  for(i=1; i<MAXSAMPLE; i++)
  { lineto(xpos,120-(long)(Resp4[i])*120/4096+ypos);
    if(++xpos>=xmax)
    { j++; xpos=0; ypos=120*j; if(ypos==360) ypos--;
        moveto(0, 120-(long)(Resp4[i+1])*120/4096+ypos); i++;
        if(j>3)
        { j=0;
          getch();
          clearviewport();
```

```
            moveto(0, 120-(long)(Resp4[i+1])*120/4096); ypos=0;
         }
      }
   }
   getch();
 /* clean up */
   closegraph();
}


void main(void)
{ Resp1ptr = Resp1;
  Resp2ptr = Resp2;
  Resp3ptr = Resp3;
  Resp4ptr = Resp4;
  ECGptr   = ECG;
  Spiroptr = Spiro;
  for(i=0; i<MAXSAMPLE; i++)
  { Resp1[i]=Resp2[i]=Resp3[i]=Resp4[i]=Spiro[i*2]=Spiro[i*2+1]=0;
    for(j=0;j<8;j++)
      ECG[i*8+j]=0;
  }
  PortNum = FIRSTPORTB;
  Direction = DIGITALOUT;
  DataValue = 0;
  cbDConfigPort (BoardNum, PortNum, Direction);
  cbDConfigPort (BoardNum, FIRSTPORTA, Direction);
  cbDOut (BoardNum, FIRSTPORTA, 10); /* RESP gain=m, TTI gain=m */
  clrscr();
  printf("\n\n\n\n\n         Allow at least 15 seconds for baseline to stabilize!");
  printf("\n\n\n       When ready .... ");
  printf("\n\n\n                   Press any key to START data acquisition .... ");
  while(!kbhit())
          { switch(i)
                { case 0:
                        DataValue = 222; /* 222 LD I, SW X*/
                        cbDOut (BoardNum, PortNum, DataValue);
                        delay (3);
                        DataValue = 223; /* 223 LD I, SW 0*/
                        cbDOut (BoardNum, PortNum, DataValue);
                        delay (7);
                        DataValue = 222; /* 222 LD I, SW X*/
                        cbDOut (BoardNum, PortNum, DataValue);
                   break;
                   case 1:
                        DataValue = 156; /* 156 LD II, SW X*/
```

```
                    cbDOut (BoardNum, PortNum, DataValue);
                    delay (3);
                    DataValue = 157; /* 157 LD, II SW 1*/
                    cbDOut (BoardNum, PortNum, DataValue);
                    delay (7);
                    DataValue = 156; /* 156 LD II, SW X*/
                    cbDOut (BoardNum, PortNum, DataValue);
            break;
            case 2:
                    DataValue = 146; /* 146 LD III, SW X*/
                    cbDOut (BoardNum, PortNum, DataValue);
                    delay (3);
                    DataValue = 147; /* 147 LD III, SW 2*/
                    cbDOut (BoardNum, PortNum, DataValue);
                    delay (7);
                    DataValue = 146; /* 146 LD III, SW X*/
                    cbDOut (BoardNum, PortNum, DataValue);
            break;
            case 3:
                    DataValue = 136; /* 136 LD IV, SW X*/
                    cbDOut (BoardNum, PortNum, DataValue);
                    delay (3);
                    DataValue = 137; /* 137 LD IV, SW 3*/
                    cbDOut (BoardNum, PortNum, DataValue);
                    delay (7);
                    DataValue = 136; /* 136 LD IV, SW X*/
                    cbDOut (BoardNum, PortNum, DataValue);
            break;
        }
            if(++i == 4) i=0;
    }
if(kbhit()) getch();        /*acquisition start*/
clrscr();
printf("\n\n\n\n\n\n\n\n        Acquiring data !");
printf("\n\n\n\n           Press any key to CANCEL data acquisition ......");
while((!kbhit())&&(Datapoint<MAXSAMPLE))
  { switch(i)
        { case 0:
        ADCIn(BoardNum, 2, 0, Spiroptr); /* read Spirometer channel */
        Spiroptr++;
        DataValue = 222; /* 222 LD I, SW X */   /* select lead & disable BLR sw */
        cbDOut (BoardNum, PortNum, DataValue);
        delay (3);
        DataValue = 223; /* 223 LD I, SW 0 */   /* enable BLR sw */
        cbDOut (BoardNum, PortNum, DataValue);
```

```
delay (2);
  ADCIn(BoardNum, 1, 0, ECGptr);        /* read ECG CH */
  ECGptr++;
delay (2);                              /* delay to center of good data */
  ADCIn(BoardNum, 0, 0, Resp1ptr);      /* read RESP1 CH */
  Resp1ptr++;
delay (3);
  ADCIn(BoardNum, 1, 0, ECGptr);        /* read ECG CH */
  ECGptr++;
DataValue = 222; /* 222 LD I, SW X */   /* disable BLR sel sw */
cbDOut (BoardNum, PortNum, DataValue);
break;                                  /* repeat for next RESP leads */
case 1:
DataValue = 156; /* 156 LD II, SW X */
cbDOut (BoardNum, PortNum, DataValue);
delay (3);
DataValue = 157; /* 157 LD, II SW 1 */
cbDOut (BoardNum, PortNum, DataValue);
delay (2);
  ADCIn(BoardNum, 1, 0, ECGptr);
  ECGptr++;
delay (2);
  ADCIn(BoardNum, 0, 0, Resp2ptr);
  Resp2ptr++;
delay (3);
  ADCIn(BoardNum, 1, 0, ECGptr);
  ECGptr++;
DataValue = 156; /* 156 LD II, SW X */
cbDOut (BoardNum, PortNum, DataValue);
break;
case 2:
  ADCIn(BoardNum, 2, 0, Spiroptr); /* read Spirometer channel */
  Spiroptr++;
DataValue = 146; /* 146 LD III, SW X */
cbDOut (BoardNum, PortNum, DataValue);
delay (3);
DataValue = 147; /* 147 LD III, SW 2 */
cbDOut (BoardNum, PortNum, DataValue);
delay (2);
  ADCIn(BoardNum, 1, 0, ECGptr);
  ECGptr++;
delay (2);
  ADCIn(BoardNum, 0, 0, Resp3ptr);
  Resp3ptr++;
delay (3);
```

```
      ADCIn(BoardNum, 1, 0, ECGptr);
      ECGptr++;
     DataValue = 146; /* 146 LD III, SW X */
      cbDOut (BoardNum, PortNum, DataValue);
    break;
    case 3:
      DataValue = 136; /* 136 LD IV, SW X */
      cbDOut (BoardNum, PortNum, DataValue);
      delay (3);
      DataValue = 137; /* 137 LD IV, SW 3 */
      cbDOut (BoardNum, PortNum, DataValue);
      delay (2);
       ADCIn(BoardNum, 1, 0, ECGptr);
       ECGptr++;
      delay (2);
       ADCIn(BoardNum, 0, 0, Resp4ptr);
       Resp4ptr++;
      delay (3);
       ADCIn(BoardNum, 1, 0, ECGptr);
       ECGptr++;
      DataValue = 136; /* 136 LD IV, SW X */
      cbDOut (BoardNum, PortNum, DataValue);
      Datapoint++;    /* last case, increment # of samples taken */
     break;
   }
   if(++i == 4) i=0;
  }
  if(kbhit()) getch();       /* end of acquisition*/
 /* plot waveform */
  plot();
  printf("\n\n\n\n\n\n\n\n         Save data to file: TRIALX.DAT ? [Y/N] ");
 scanf("%c",&ch);
 if((ch=='y')|| (ch=='Y'))
 { /* open file and save data in file */
  if ((out = fopen("TRIALX.DAT", "wt"))== NULL)
  { printf("Cannot open TRIALX.DAT file.\n");
  }
  else
  { /*fprintf(out,"Spiro Resp1 Resp2 Resp3 Resp4 ECG\n");*/ /*OPTIONAL TITLE
 FOR EACH COLUMN*/
    fprintf(out,"%-7d%-7d%-7d%-7d%-7d%-7d%-7d%-7d%-7d%-7d%-7d%-7d%-
 7d",
               MAXSAMPLE,0,0,0,0,0,0,0,0,0,0,0,0);
   fprintf(out,"\n");
   for(i=0; i<MAXSAMPLE; i++)
```

```
{ fprintf(out,"%-7d%-7d%-7d%-7d%-7d%-7d",
              Spiro[i*2],Spiro[i*2+1],Resp1[i],Resp2[i],Resp3[i],Resp4[i]);
    for(j=0;j<8;j++)
      fprintf(out,"%-7d",ECG[i*8+j]);
    fprintf(out,"\n");
  }
  fclose(out);
  }
 }
}
```

MATLAB PROGRAMS

% RUNTRIAL.M

% This is the main batch program for the MATLAB programs

```
clear all;
load c:\path\trial**.dat;
trial=trial**;
clear trial**;
pack;
sprun;
iprun;
ecgrun;
clear trial
pack
save trial**;
ipmean**=ipmean;
spvol**=spvol;
rm**=rm;
save cordat40 ipmean40 spvol40 rm40;
%corrplot;
clear all;
pack;
%end
```

% SPRUN.M
% This is the batch program for the spirometer
% signal processing programs.

```
spload;
sprange;
spindex;
spvol;
%clear spiro;
clear sprange;
pack;
%end
```

```
%      SPLOAD.M
%      THIS PROGRAM LOADS THE SPIROMETER DATA FROM TWO
%      COLUMNS ANS SCALES IT.
maxsample=trial(1,1);      % loads number of samples per column from data
spiro=zeros((maxsample)*2,1);          % initalizes spiro to one column
for i=1:(maxsample),                    % trial row 1 is invalid
    spiro((i*2)-1)=trial(i+1,1)/409.6-5.0; % loads and scales data by
    spiro(i*2)=trial(i+1,2)/409.6-5.0;    % alternating columns
end
spsample=maxsample*2;      % defines total number of spiro samples
for i=1:spsample,
    if spiro(i,1)>2        % scales data to 1 or 0 based on a threshold
        spiro(i,1)=1;
    else
        spiro(i,1)=0;
    end
end
%end of program




% SPRANGE.M
% THIS PROGRAM FINDS THE RANGES OF INSPIRATION (0)
% AND EXPIRATION (1) OF THE SPIROMETER DATA.
sprange=zeros(spsample,1);
sprange(1,1)=spiro(1,1);          % initalize first data point
k=0;
for i=1:(spsample-51),
    if (spiro(i) + spiro(i+1))==1  % true = transition
        for j=1:50,                % tests over the next 1 sec. of data
        if (spiro(i+1) + spiro(i+1+j))==1
            k=(k+1);
          else
          end
        end
        if k==0
          sprange(i+1)=0;       % Transition to inspiration.
        else
          sprange(i+1)=1;       % Transitions detected.
          k=0;
        end
    else
        sprange(i+1)=sprange(i);   % No transition.
    end
end
%end of program
```

% SPINDEX.M
% THIS PROGRAM INDEXES EACH SPIROMETER BREATH AND ITS ASSOCIATED
% INSPIRATION AND EXPIRATION.

```
bn=0;                           % initialize breath number
for i=3:spsample-52,
    if sprange(i) + sprange(i+1)==1 % tests for transition in range
        if sprange(i+1)==0
            bn=bn+1;
            spinstart(bn)=i+1;  % finds start of inspiration
        elseif bn>0
            spexstart(bn)=i+1;  % finds start of expiration
        else                    % skips if first insp not found yet
        end
    else
    end
end
totalnb=bn-1;                   % total valid breaths indexed
for j=1:bn-1,
    spinend(j)=spexstart(j);    % finds end of inspiration
    spexend(j)=spinstart(j+1);  % finds end of expiration
end
% end of program.
```

% SPVOL.M
% THIS PROGRAM COUNTS THE SPIROMETER EXPIRATION TRANSITIONS
% AND CACULTAES THE VOLUME FOR EACH BREATH IN SPIRO USING
% INDEXES FROM INDEX.
%bn = breath number
%totalnb = total number of breaths

```
spvol=zeros(totalnb-1,1);
for bn=1:totalnb-1,
    count(bn)=0;
    for i=(spexstart(bn)-2):(spexend(bn)+2),
        if spiro(i) + spiro(i+1)==1      % tests for transition
            count(bn) = count(bn)+1;
        else
        end
    end
    spvol(bn)=count(bn)*0.05;  % vol=# of transitions x .05L
end
```

% end of program.

```
% IPRUN.M
ipload;
ipinterp;
ipfilt;              % filtered data (comment out for unfiltered)
ipindex;
clear ipx;
ipdiff;
%ipcomp;
ipmean;
pack;
```


```
% IPLOAD.M
% THIS PROGRAM  EXTRACTS THE RESPIRATION LEADS
% FROM THE RAW ACQUIRED DATA AND AND SCALES THE DATA TO +/-5V.


maxsample=trial(1,1);        % loads number of samples per column from data
ip1=zeros((maxsample),1);
ip2=zeros((maxsample),1);
ip3=zeros((maxsample),1);
ip4=zeros((maxsample),1);
for i=1:(maxsample),               % trial row 1 is invalid
    ip1(i)=trial(i+1,3)/409.6-5.0;       % input ip data and scale
    ip2(i)=trial(i+1,4)/409.6-5.0;
    ip3(i)=trial(i+1,5)/409.6-5.0;
    ip4(i)=trial(i+1,6)/409.6-5.0;
end
pack;
% end of program
```


```
% IPINTERP.M
% THIS PROGRAM INTERPOLATES THE IP DATA TO 2X THE
% NUMBER OF SAMPLES TO MATCH THE SPIRO DATA.
ip1=interp(ip1,2);
ip2=interp(ip2,2);
ip3=interp(ip3,2);
ip4=interp(ip4,2);

% end of program
```

% IPFILT.M
% THIS PROGRAM FILTERS THE SCALED IP DATA.

```
[b,a]=butter(1,0.25);          % 2-pole LPF (1 each direction), 6.25Hz.
ip1=filtfilt(b,a,ip1);
ip2=filtfilt(b,a,ip2);
ip3=filtfilt(b,a,ip3);
ip4=filtfilt(b,a,ip4);


% end of program
```

% IPINDEX.M
% THIS PROGRAM FINDS THE IP EXPIRATION START AND END DATA, AND
%THEIR INDEXES FOR EACH BREATH FOR EACH SET OF IP LEAD DATA.

```
for x=1:4,
   if x==1                    % ip lead 1
     ipx=ip1;
   elseif x==2                % ip lead 2
     ipx=ip2;
   elseif x==3                % ip lead 3
     ipx=ip3;
   elseif x==4                % ip lead 4
     ipx=ip4;
   end
   for bn=1:totalnb-1,        % last breath is not valid
     y1=ipx(spexstart(bn));
     y2=ipx((spexstart(bn))+10);
       if y1>y2                % tests for polarity inversion
         [y,i]=max(ipx(spinstart(bn):spinstart(bn+1)));
         [z,j]=min(ipx(spexstart(bn):spexstart(bn+1)));
       else                              % finds max & min
         [y,i]=min(ipx(spinstart(bn):spinstart(bn+1)));
         [z,j]=max(ipx(spexstart(bn):spexstart(bn+1)));
       end
       if x==1
         ip1exstdata(bn)=y;            % stores indexes for each breath
         ip1exstart(bn)=i+spinstart(bn);
           ip1exendata(bn)=z;
         ip1exend(bn)=j+spexstart(bn);
         elseif x==2
         ip2exstdata(bn)=y;
```

```
        ip2exstart(bn)=i+spinstart(bn);
            ip2exendata(bn)=z;
        ip2exend(bn)=j+spexstart(bn);
        elseif x==3
        ip3exstdata(bn)=y;
        ip3exstart(bn)=i+spinstart(bn);
            ip3exendata(bn)=z;
        ip3exend(bn)=j+spexstart(bn);
        elseif x==4
        ip4exstdata(bn)=y;
        ip4exstart(bn)=i+spinstart(bn);
            ip4exendata(bn)=z;
        ip4exend(bn)=j+spexstart(bn);
        end
    end
end


% end of program.



% IPDIFF.M
% THIS PROGRAM CALCULATES THE DIFFERENCE IPEXSTDATA -
% IPEXENDATA
% AND DECLARS THIS TO BE IP#DIFF.  THIS IS DONE FOR EACH BREATH
% IN EACH OF THE IP LEADS.

    bn=0;                         % breath number
    for bn=1:totalnb-1,
        ip1diff(bn)=abs(ip1exstdata(bn)-ip1exendata(bn));
    end
    for bn=1:totalnb-1,
        ip2diff(bn)=abs(ip2exstdata(bn)-ip2exendata(bn));
    end
    for bn=1:totalnb-1,
        ip3diff(bn)=abs(ip3exstdata(bn)-ip3exendata(bn));
    end
    for bn=1:totalnb-1,
        ip4diff(bn)=abs(ip4exstdata(bn)-ip4exendata(bn));
    end
ip1diff=ip1diff(:);
ip2diff=ip2diff(:);
ip3diff=ip3diff(:);
ip4diff=ip4diff(:);

% end of program.
```

```
% ECGRUN.M
ecgload;
ecgfilt;          % comment out for unfiltered

%end of program


% ECGLOAD.M
% THIS PROGRAM LOADS THE ECG DATA FROM EIGHT COLUMNS AND
SCALES IT.
maxsample=trial(1,1);    % loads number of samples per column from data
ecg=zeros((maxsample)*8,1);          % initalizes ecg to one column
for i=1:(maxsample),
    for j=1:8,                          % trial row1 data is invalid
        ecg((i*8)+j-8)=trial(i+1,6+j)/409.6-5.0; % loads and scales data
    end
end

%end of program
% ECG FILT.M
% THIS PROGRAM FILTERS THE ECG DATA

[b,a]=butter(1,0.5);          % 2-pole LPF (1 each direction), 50Hz.
ecg=filtfilt(b,a,ecg);


% IPMEAN.M
ipmean=zeros(totalnb-1,1);
for i=1:totalnb-1,
    ipmean(i)=((ip1difff(i))+(ip2difff(i))+(ip3difff(i))+(ip4difff(i)))/4;
end

% end of program
```

S-Plus Functions

To scan in a 1column by x row ASCII matrix,:

*output*_matrix(scan("*path/*_data*input filename*",)ncol=1,byrow=T

To call the GAM or GLM function:

*result*_gam(*standard data*~s(*data1*)+s(*data2*)+s(*data3*)+s(*data4*)

The transfer functionm "s" (spline) can be substituted with p (poly), lo (loess) or no function.

To obtain residual deviances, type *result.*

To "extract" model data use:

fitted*(result)*

residuals*(result)*

coefficients*(result)*

To write data in S-Plus to an ASCII file:

write(round(data,#),"*output name*",ncol=1)

= the number of digits to round to

REFERENCES

[1] K. Cheng, S. J. Simske, D Isaacson, J. C. Newell and D. G. Gisser, "Errors Due to Measuring Voltage on Current-Carrying Electrodes in Electric Current Computed Tomography." IEEE Trans. Biomed. Eng., 1990, vol. 37, pp. 60-65.

[2] A. C. Guyton, *Textbook of Medical Physiology*. Philadelphia: W. B. Saunders, 1986.

[3] L. H. Hamilton, "Transthoracic Impedance Measurements of Ventilation in Adults and Children." Physiological Applications of Impedance Plethysmography, Ninth National ISA Biomedical Symposium, 1971, pp. 99-118.

[4] D. J. Hansen, L. V. M. Troy R. A. Deininger and T. K. Collopy, "Computer Assisted Spirometry." Am. Ind. Hyg. Assoc. J., 1983, 44(6), pp. 419-424.

[5] D. J. Hansen, L. W. Whitehead and J. A. Foulke, "Computerized Spirometry Using a Portable Microcomputer." Am. Ind. Hyg. Assoc. J., 1985, 46(7), pp. 373-378.

[6] P. Hua, E. J. Woo, J. G. Webster and W. J. Tompkins, "Using Compound Electrodes in Electrical Impedance Tomography." IEEE Trans. Biomed. Eng., 1993, vol. 40, pp. 29-34.

[7] M.V. Kamath and E.L. Fallen, "Power Spectrical Analysis of Heart Rate Variability: A Noninvasive Signature of Cardiac Autonomic Function." Critical Rev. Biomed. Eng., 1993, vol. 21(3), pp. 245-311.

[8] S. Luo, V.X. Afonso, J.G. Webster and W.J. Tompkins, "The Electrode System in Impedance-Based Ventilation Measurement." IEEE Trans. Biomed. Eng., 1992, vol. 39, pp. 1130-1141.

[9] J. Nyboer, "Bio-Ohemic Sensing." Physiological Applications of Impedance Plethysmography, Ninth National ISA Biomedical Symposium, 1971, pp. 21-30.

[10] A.F. Pacela, "Impedance Pneumography-a Survey of Instrumentation Techniques." *Med. & biol. Engng.*, 1966, Vol. 4, pp.1-15.

[11] J. Rosell, J. Colominas, P. Riu, R. Pallas-Areny and J.G. Webster, "Skin Impedance from 1Hz to 1MHz." IEEE Trans. Biomed. Eng., 1988, vol. 35, pp. 649-651.

[12] A. V. Sahakian, W. J. Tompkins and J. G. Webster, "Electrode Motion Artifacts in Electrical Impedance Pneumography." IEEE Trans. Biomed. Eng., 1985, vol. BME-32, pp. 448-451.

[13] K. Seshadri, *Correlation Between Tidal Volume Measured by Spirometry and Impedance Pneumography.* Masters thesis, NJIT, October 1994.

[14] M. Smith, "Rx for ECG Monitoring Artifact." Reprint from Critical Care Nurse, 1984, vol. 4, N0.1.

[15] A. J. Vander, J. H. Sherman and D. S. Luciano, *Human Physiology - The Mechanisms of Body Function.* New York: McGraw-Hill, 1985.

[16] R. Wadhwani and R.L. Longini, "Analysis of Quiet Spontaneous Breathing as Measured by Spirometer and Electrical Impedance Plethysmograph." Computers and Biomedical Research, 1973, 6 pp. 74-89.

[17] K. Yana, J. P. Saul, R. D. Berger, M. H. Perrott, and R J. Cohen, "A Time Domain Approach for the Fluctuation Analysis of Heart Rate Related to Instantaneous Lung Volume." IEEE Trans. Biomed. Eng., 1993, vol. 40, pp. 74-81.

[18] P. Zhang, *Heart Rate Variability Study Using Phase Response Curve.* Doctoral dissertation, NJIT, May 1994.